Pulmonary and Extrathymic Mediastinal Tumors

Karen Lyons, R. Paul Guillerman, and Kieran McHugh

Contents

Abstract

The most frequently encountered pediatric thoracic tumors are pulmonary metastases from extracranial solid tumors. Primary pulmonary neoplasms are rare in childhood, but can cause considerable morbidity and mortality from mass effect, tissue invasion, and metastatic disease in affected children. Mesenchymal neoplasms are more common than epithelial neoplasms in the pediatric lung, unlike in adults, and some of these neoplasms are associated with predisposing genetic syndromes and certain infections. While lymphoma is the most common mediastinal malignancy, germ cell, neuroblastic, and other mediastinal tumors also manifest with distinctive features that are important to recognize for appropriate management. Many of these tumors are detectable on chest radiography, but chest CT remains the primary imaging modality used to formulate a differential diagnosis for these tumors, define anatomy for preoperative planning, assess tumor response to therapy, and survey for recurrent disease, with MRI and nuclear medicine studies playing a complementary role. This chapter will review the characteristic clinical presentations and imaging findings of selected pulmonary and extrathymic mediastinal tumors of childhood.

1 Introduction

Thoracic tumors are often classified, despite some overlap, as originating in one of three major thoracic compartments, namely the lungs, the mediastinum, or the chest wall. In the interests of simplicity and convention, this anatomical approach will be used in this chapter, with the focus on tumors of the lungs and certain tumors of the mediastinum. In this book, lymphoma and thymic tumors are covered in the chapter entitled Imaging Evaluation of the Thymus and Thymic Disorders in Children by Sams and Voss, and chest

K. Lyons · R. Paul Guillerman (✉)
Department of Pediatric Radiology,
Texas Children's Hospital,
Baylor College of Medicine,
6701 Fannin St, Suite 470,
Houston, TX 77030, USA
e-mail: rpguille@texaschildrens.org

K. McHugh
Department of Radiology,
Great Ormond Street Hospital for Children NHS Trust,
Great Ormond Street, London, WC1N 3JH, UK
e-mail: Kieran.McHugh@gosh.nhs.uk

P. Garcia-Peña and R. P. Guillerman (eds.), *Pediatric Chest Imaging*, Medical Radiology. Diagnostic Imaging,
DOI: 10.1007/174_2014_960, © Springer-Verlag Berlin Heidelberg 2014
Published Online: 21 February 2014

wall tumors, hemangiomas, lymphatic malformations, and neurofibromas are covered in the chapter entitled Radiology of the Chest Wall by Eich, Kellenberger and Willi, and will not be further addressed in this chapter. An emphasis is placed on imaging features of these thoracic tumors at diagnosis. The subsequent follow-up imaging of benign conditions is governed by the clinical course, and that of malignancies is largely determined by protocols devised by the various pediatric oncology co-operative groups.

2 Clinical Features

The most frequently encountered pediatric thoracic tumors, particularly in pediatric oncology centers, are pulmonary metastases. These are usually initially found during staging of a known or suspected malignancy and the dominant clinical findings are typically those related to the primary tumor. Primary thoracic neoplasia is uncommon in childhood and seldom an early diagnostic consideration, but a wide variety of tumors do occur within the chest and appropriate management is facilitated by correct recognition on imaging. There is no major difference between the sexes in the incidence of primary chest tumors, and tumors occur with relatively equal frequency in either lung.

Primary chest neoplasms largely manifest either due to pressure effects from compression of adjacent organs, systemic symptoms from disseminated malignancy, or as an incidental finding. Paraneoplastic syndromes are very rare, and usually limited to neuroblastoma or bronchial carcinoid. In the setting of airway obstruction or respiratory symptoms that do not respond to conventional medical treatment, computed tomography (CT) can be very useful in demonstrating a mass lesion occult to chest radiography (CXR). While the presenting symptoms can vary greatly even within the same histological group, some generalizations with regard to the presentation of chest masses can be made.

In both benign and malignant lung tumors, the most frequent presenting complaints are fever, cough, and pneumonitis (Hancock et al. 1993; Hartman and Shochat 1983). Hemoptysis and respiratory distress are more common with malignant pulmonary lesions. In the largest review series to date, 28 % of benign tumors were asymptomatic as compared to 6 % of malignant tumors (Hancock et al. 1993). A child who is truly asymptomatic is twice as likely to harbor a benign pulmonary tumor, and this likelihood is even greater in children over 4 years of age. Endobronchial masses typically result in lung collapse, persistent hyperinflation, or wheezing which fails to respond to conventional treatment and may be complicated by bronchiectasis. The endobronchial location of many such lesions may be apparent only after careful review of multiplanar CT images or bronchoscopy.

Thoracic neurogenic tumors such as neuroblastoma and ganglioneuroma are often found incidentally on a CXR performed for other reasons, while the majority of mediastinal tumors generally present with respiratory symptoms such as airway obstruction, cough, or fever due to a complicating pneumonia. In contrast to many tumors of pulmonary origin, the likely nature of the illness is apparent on CXR. The opacity is generally not typical for pneumonia with often clearly defined margins suggesting an extrapulmonary origin. Mediastinal shift or adenopathy may be seen and rib destruction, in particular, should be sought as this latter finding virtually always indicates an extrapulmonary malignancy. In fact, the majority of mediastinal and chest wall tumors seen in children are malignant.

3 Imaging

CXR remains the most common initial imaging modality for evaluation of chest masses secondary to its wide availability, low cost, and relatively low associated radiation dose. Radiological investigation should begin with a frontal CXR. When an unusual opacity is evident, a lateral view can be particularly helpful in assessing the trachea for compression and/or displacement, and in accurately defining the location of the abnormality, which aids greatly in establishing a differential diagnosis. Chest CT is used to investigate suspicious or persistent abnormalities seen on CXR, or to detect disease occult on CXR. Compared to CXR, CT is much more sensitive for detecting small lesions and calcifications, and better at defining anatomic relationships and mass effect on critical structures such as the airway and great vessels. Due to its greater sensitivity for small lesions and precision for measuring the size of lesions, CT is routinely used in follow-up of treated malignancy. While CT is highly sensitive, it lacks specificity and cannot reliably differentiate between benign and malignant lung nodules (McCarville et al. 2006; Silva et al. 2010). Correlation with clinical history and serial imaging follow-up improves its specificity. CT is also useful for guiding tissue sampling.

Contemporary multidetector volumetric CT scanners can acquire images of the entire chest of a child within a few seconds or even less than a second, resulting in less need for sedation and less motion artifact (Bastos et al. 2009). These scanners also allow generation of high-resolution multiplanar reconstructions (MPR) and 3D renderings to better depict anatomy for diagnostic and treatment planning. The dose of ionizing radiation from CT is typically much higher than from CXR, but can be reduced without compromising image quality by judicious application of new techniques such as iterative reconstruction (Brady et al. 2014). To better characterize tumors and evaluate the mediastinal/hilar

Table 1 Spectrum of benign and malignant primary pediatric tumors

Primary Pulmonary Tumors	
Benign	Malignant
Hamartoma	Inflammatory myofibroblastic tumor
Chondroma	Pleuropulmonary blastoma
Fetal lung interstitial tumor	Bronchial carcinoid
Infantile myofibromatosis	Mucoepidermoid carcinoma
Congenital peribronchial myofibroblastic tumor	NUT midline carcinoma
Papilloma	Bronchogenic carcinoma
Leiomyoma	Leiomyosarcoma

structures, intravenous contrast is typically administered for chest CT scans of primary thoracic tumors for initial staging, therapy response assessment, and relapse surveillance. However, chest CT scans performed to detect and follow-up lung metastases from extrathoracic nonlymphomatous tumors can be performed without intravenous contrast (Kuhns and Roubal 1995) at relatively low tube current (Diederich et al. 1999) without loss of sensitivity because of the high inherent contrast of aerated lung parenchyma. Use of maximum intensity projection (MIP) images can improve sensitivity for small pulmonary nodules (Coakley et al. 1998; Kawel et al. 2009). Maximum intensity projection (MIP) processing has several advantages in the detection of small nodules: vascular structures appear as tubular and branching structures rather than as discrete nodules; the MIP slab preserves the inherent resolution of the original images; MIP images can be constructed in any plane; and image numbers are markedly reduced in comparison to the axial image set from a routine MDCT study (Gruden et al. 2002). Use of MIP images should complement but not substitute for axial image review. Computer-aided detection (CAD) has been shown to have good sensitivity for detection of nodules 4 mm in diameter or larger with a low false positive rate (Helm et al. 2009), but is not in widespread use in pediatric imaging. In routine clinical practice, contiguous axial sections are usually adequate for nodule detection, supplemented by coronal or sagittal reformatted images for decision making on questionable small nodules.

CT virtual bronchoscopy (VB) can better define the endobronchial anatomy when an endobronchial lesion is present. The added value of this information is questionable, however. VB can increase total examination time and cost, and may not provide additional clinically useful information over MPR images (Kocaoglu et al. 2006). Despite meticulous technique and attention to detail, postobstructive pneumonitis, or atelectasis may obscure an endobronchial tumor, resulting in a false negative CT study.

CT after intravenous contrast administration can accurately define mediastinal masses and is sensitive in the detection of adjacent bony destruction from chest wall masses. Magnetic resonance imaging (MRI), however, has become the preferred technique for examining chest wall masses, and in some cases, mediastinal masses. This has come about mainly as a result of faster scanning sequences, improved gating techniques to reduce cardiorespiratory motion artifact, and MR angiography to better depict the vasculature, in addition to the conventional advantages of better soft-tissue contrast and lack of ionizing radiation exposure compared to CT (Newman 2011). Most tumors have intermediate or low signal intensity on T1-weighted sequences, are hyperintense to varying degrees on T2-weighted sequences, and display variable contrast enhancement after gadolinium administration. Rather than actual signal characteristics, it is the site of tumor occurrence and the age of the patient that suggests the most likely tumor in an individual case.

The role of FDG-PET in evaluating nonlymphomatous chest tumors has yet to be clearly established. There may be a limited role for FDG-PET in improving the specificity for malignancy in enlarged lymph nodes or lung nodules visualized on CT (Kleis et al. 2009; Cistaro et al. 2012).

4 Pulmonary Tumors

Primary pulmonary neoplasms are unusual in childhood, and far less common than non-neoplastic, mass-like processes. The absence of pyrexia or leukocytosis helps exclude a round pneumonia, lung abscess, or infected congenital pulmonary airway malformation (CPAM). Clinical history and laboratory tests are often valuable in suggesting granulomatous disease, infarction, or hematoma as a cause of pulmonary mass. Metastases from an extrapulmonary primary malignancy are far more common than

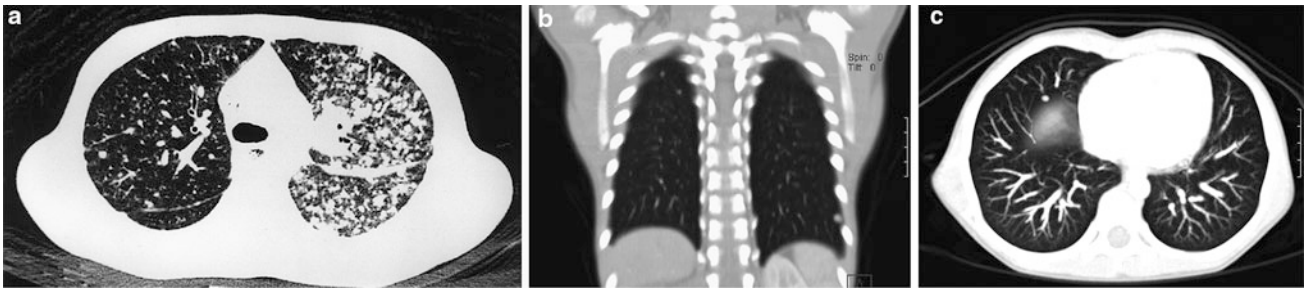

Fig. 1 Pulmonary metastases. **a** Axial chest CT image demonstrates predominantly left-sided pulmonary nodularity, pleural and interstitial thickening due to neuroblastoma metastases. An unusual lymphatic pattern of tumor spread has occurred in this patient. **b** Two subtle right apical pulmonary nodules and another nodule in the left lower lobe depicted on a coronal CT image are suspicious for metastatic disease in a different 4-year-old patient with a newly diagnosed renal tumor. **c** Axial MIP CT image from the same patient illustrating how the MIP technique clearly helps differentiate between pulmonary vessels and small lung nodules

primary pulmonary tumors in children (Cohen and Kaschula 1992). A majority (76–88 %) of primary pulmonary tumors in childhood are malignant (Hancock et al. 1993) (Table 1).

4.1 Pulmonary Metastases

The lungs are a common site of metastatic spread of many pediatric solid extracranial malignancies, including (with an approximate percentage incidence of pulmonary metastases at diagnosis) Wilms tumor (10 %), osteosarcoma (15–20 %), Ewing sarcoma (15–20 %), rhabdomyosarcoma (15 %), and hepatoblastoma (10 %) (Paulussen et al. 1998; Kaste et al. 1999). Pulmonary metastases are found in only 1–3 % of cases of neuroblastoma at diagnosis (Cowie et al. 1997), and in 3–4 % of those with stage 4 disease (DuBois et al. 2008), but are a prognostic marker of unfavorable outcome (Kammen et al. 2001; DuBois et al. 2008), as is the case for nearly all pediatric solid extracranial malignancies (Fuchs et al. 2012). Routine chest CT for staging purposes is warranted at diagnosis for these malignancies, as well as for some other less common pediatric malignancies. Staging for metastatic neuroblastoma is, however, best achieved with metaiodobenzylguanidine (MIBG) scanning. Lung metastases usually result from hematogenous dissemination and manifest as multiple, well-defined pulmonary nodules. Lymphatic spread producing a reticular or reticulonodular pattern can also occur in neuroblastoma (McCahon 2006) (Fig. 1).

Diagnostic dilemmas arise when pulmonary nodules are small (a few millimeters in diameter), indistinct, or solitary. Among malignant causes, an incidentally detected nodule is much more likely to represent a metastasis rather than a primary lung tumor in a child. Benign causes of pulmonary nodules are myriad and include granulomas (particularly in areas with a high prevalence of histoplasmosis or tuberculosis), hamartomas, chondromas, intraparenchymal lymph nodes, septic emboli, plugged distal airways, previous varicella infection, vasculitis, Langerhans cell histiocytosis,

Fig. 2 Intrapulmonary lymph node. Axial chest CT image from a 17-year old with osteosarcoma undergoing staging demonstrates a well-circumscribed, bean-shaped, solid pulmonary nodule (*arrow*) of the right lower lobe close to the pleura. This nodule proved to be an intrapulmonary lymph node rather than a metastasis upon biopsy

respiratory papillomatosis, opportunistic infections in the setting of immunodeficiency, and fibrotic nodules in the setting of bleomycin or cyclophosphamide toxicity. Clustering of multiple nodules favors an infectious or inflammatory etiology. Spontaneous resolution of pulmonary nodules may be related to a focal inflammatory process, atelectasis, mucoid impaction of small bronchi, or intermittent enlargement of benign intrapulmonary lymph nodes (Diederich et al. 2005). Intrapulmonary lymph nodes tend to be located peripherally below the level of the carina at or near the junction of the pleura and adjacent lung lobules (Wang et al. 2013) (Fig. 2).

In an individual case, it can be very difficult to distinguish benign from metastatic pulmonary nodules in young patients with a solid extracranial malignancy. A study of pediatric oncology patients found that the most significant predictors of a pulmonary nodule being metastatic were peripheral location, size between 5 and 10 mm diameter, location in the right lower lobe, and a history of osteosarcoma, Ewing sarcoma, or hepatocellular carcinoma

(Murrell et al. 2011). Another study found that sharp nodule margins and development of new nodules are significantly associated with malignancy, but that nodules measuring less than 5 mm in diameter are as likely to be malignant as larger nodules, unlike in adults (McCarville et al. 2006). Co-existence of both benign and malignant nodules is also possible. In the setting of pediatric osteosarcoma, over 90 % of malignant nodules are correctly classified, while only 11–30 % of benign nodules are correctly classified on the basis of imaging findings (Brader et al. 2011).

FDG-PET may be a useful adjunct for the evaluation of possible pulmonary metastases in pediatric malignancies. FDG-PET confers significantly higher specificity than CT for pulmonary metastases greater than 5 mm diameter in children (Kleis et al. 2009). A prospective study of FDG-PET/CT in the characterization of pulmonary nodules in children with bone sarcoma demonstrated a sensitivity of 90 % and specificity of 94 % using a SUV_{max} value around 1, compared to a sensitivity of 90 % and specificity of 81 % using a cut-off value of 6 mm for nodule diameter (Cistaro et al. 2012).

Findings equivocal for pulmonary metastatic disease on chest CT warrant further evaluation, either with FDG-PET, close surveillance with follow-up imaging, or biopsy. Because of the survival advantage conferred by complete resection of pulmonary metastases in selected pediatric malignancies (Tronc et al. 2008) and the difficulty in reliably diagnosing metastatic disease solely by imaging when only one or a few small lung nodules are discovered in a child with a solid tumor, there is a trend toward resecting or performing a biopsy of indeterminate pulmonary nodules. Fine needle aspiration cytology is widely practiced in adult patients with carcinoma and is usually diagnostic. In children, however, sarcomas are much more common, and aspiration cytology is generally regarded as unreliable for the diagnosis of childhood tumors since differentiation from other cells can be extremely difficult on small cytological specimens and architectural information is lost. Core needle biopsies of small pulmonary nodules in children under CT guidance using a co-axial system permit multiple biopsies through a single pleural pass to be obtained, yielding adequate tissue for diagnosis in most cases and reducing the likelihood of complicating hemothorax or pneumothorax (Connolly et al. 1999).

A successful response to chemotherapy should be accompanied by disappearance of pulmonary metastases. Occasionally, nodules may demonstrate incomplete resolution related to residual fibrosis or selection of less mitotically active cells (as in the case of rhabdomyomatous differentiation in Wilms tumors or mature teratoma elements in germ cell tumors), but ultimately proof of a benign nature rests on either biopsy or stability on follow-up, particularly off treatment (Seemayer et al. 1997; Seifert et al. 2012). If the initial chest CT at diagnosis is negative for metastases, later follow-up for pediatric oncology patients is largely with CXR, with CT reserved for equivocal CXR findings, clinically suspected relapses, or tumors with a high risk of pulmonary relapse.

Patients with osteosarcoma or FDG-PET positive disease at initial presentation appear to be at the highest risk of recurrent pulmonary metastatic disease (Murrell and Dasgupta 2013). As up to 30–40 % of children with osteosarcoma eventually develop pulmonary metastases and complete surgical remission is the main prognostic factor affecting survival, routine chest CT surveillance, and pulmonary metastasectomy of osteosarcoma patients may be justified (Diemel et al. 2009). In an osteosarcoma patient, pulmonary nodules, particularly those that are calcified or greater than 5 mm in diameter, should be regarded as malignant until proven otherwise (McCahon 2006; Brader et al. 2011). CT also tends to underestimate the number of metastatic pulmonary nodules found at thoracotomy in osteosarcoma patients (Kayton et al. 2006). Centrally-located pulmonary metastases of osteosarcoma may be associated with reduced median survival compared with those that are peripherally sited (Letourneau et al. 2011). Osteosarcoma may also metastasize to the mediastinal lymph nodes and pleura, and even to the myocardium. Cavitary metastases are unusual in childhood but are occasionally seen with sarcomas or Wilms tumor, or after chemotherapy or radiotherapy.

Co-operative pediatric oncology groups in North America and Europe once recommended that presumed pulmonary metastases from Wilms tumor could be ignored if they were not visible on CXR. This is no longer the case with current protocols from the Children's Oncology Group (COG) and the International Society of Pediatric Oncology (SIOP). However, the clinical significance of these small nodules that are detectable only with CT in patients with Wilms tumor is uncertain. A retrospective review of National Wilms Tumor Studies (NWTS)-4 and -5 found that patients with pulmonary nodules detected only by CT who received three chemotherapeutic agents had improved 5 year event-free survival, but not overall survival, compared with those receiving only two drugs (Grundy et al. 2012). These so-called CT-only patients represent a small (2–4 %) cohort of all Wilms patients (Smets et al. 2012). It has been argued that this small proportion of CT-only detected lesions makes it difficult to justify the routine use of a relatively high radiation technique such as CT when patient outcomes may not be affected by the CT findings in the setting of Wilms tumor (Smets et al. 2012). In a SIOP Wilms study, patients with CT-only lesions should have been treated as having localized disease but many were not, leading the authors to conclude that current clinical decision-making was based on a fear of under-treatment. The outcome for patients with CT-only lesions, whether treated

as localized or metastatic disease (the latter received more intensive therapy), were no different. Some patients with CT-only lesions may have benign chest disease, yet suffer late toxic effects from more intensive therapy. This underscores the need to devise better diagnostic imaging tests for the detection of metastases and selection of patients for more intensive therapy. Chest CT perhaps could be used in children with Wilms tumor after preoperative chemotherapy and nephrectomy to select those with persisting pulmonary lesions. The finding of persisting pulmonary lesions in combination with high risk histology and/or stage III disease confers a worse prognosis, and therefore these patients might benefit from intensified therapy (Smets et al. 2012). Wilms tumor patients with metastatic lung disease at presentation who are in complete pulmonary remission after chemotherapy with or without metastasectomy have a better outcome than those with unresectable pulmonary metastases. The findings on chest CT help determine which patients should or should not receive radiotherapy, with persisting lung lesions being an indication for radiotherapy (Verschuur et al. 2012).

An aggressive diagnostic approach with chest CT is also advocated in pediatric malignant non-Wilms renal tumors, where survival requires complete clearance of lung metastases, either through chemotherapy, radiotherapy, or metastasectomy (Warmann et al. 2012).

4.2 Pulmonary Lymphoma and Post-transplantation Lymphoproliferative Disorder

Pulmonary involvement occurs in approximately 10 % of cases of pediatric lymphoma and is usually associated with ipsilateral hilar or mediastinal lymphadenopathy. Pulmonary lymphoma is most frequently seen in Hodgkin disease or anaplastic large cell non-Hodgkin lymphoma, and most often manifests as nodules or consolidative masses. A reticular pattern related to lymphatic spread can also be observed (Maturen et al. 2004). In the setting of pediatric Hodgkin lymphoma, direct contiguous involvement of the lung by an adjacent mediastinal mass is considered stage IIE invasive disease rather than disseminated stage IV disease (Guillerman et al. 2011).

Post-transplantation lymphoproliferative disorder (PTLD) is thought to result from an Epstein–Barr virus (EBV)-induced proliferation from B-cell lymphocytes, which is normally opposed by a functioning T-cell system in immunocompetent patients. It is estimated to occur in 2–3 % of all solid organ transplants including both children and adults, but the incidence in children with lung transplants is reported to be 8 % (Pickhardt et al. 2000). Post-transplantation lymphoproliferative disorder (PTLD) occurs more often and presents earlier in lung transplants compared with other solid organ transplants, with a median time from transplant to diagnosis of 6–10 months (Wilde et al. 2005; Siegel et al. 2003). The overall prevalence of pulmonary involvement in pediatric PTLD is 29 % (Maturen et al. 2004), and a large majority of pediatric lung transplant recipients with PTLD have intrathoracic involvement of the lungs or mediastinum (Wilde et al. 2005).

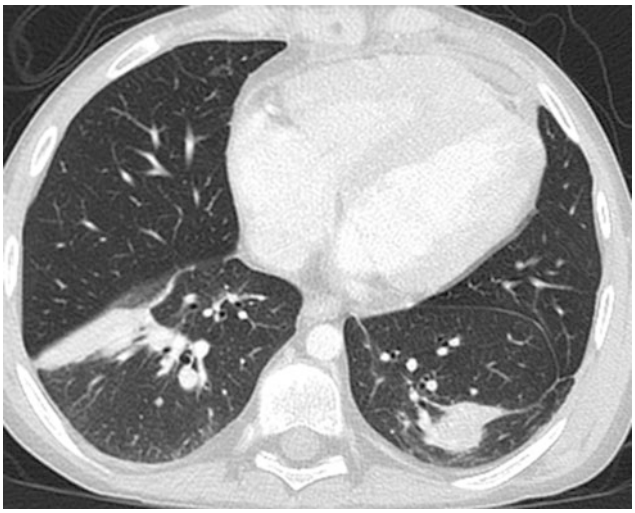

Fig. 3 Post-transplantation lymphoproliferative disorder (PTLD). Axial chest CT image from a 15-year-old post lung transplantation demonstrates lobular subsegmental masses of the lower lobes. Biopsy revealed monomorphic PTLD, diffuse large B-cell lymphoma type

The most common presentation of intrathoracic PTLD is asymptomatic pulmonary nodules. Close monitoring of EBV viral load and the degree of immunosuppression via lymphocyte function assays can facilitate an early diagnosis (Elidemir et al. 2009). Children at greatest risk are those who receive EBV-positive donor lungs who were EBV-seronegative prior to transplantation. The typical CT appearance is multiple well-defined, soft-tissue attenuation pulmonary nodules measuring 1–4 cm. They are usually homogeneous but can have central necrosis. In approximately 10 % of cases, multifocal masses or consolidations are the predominant parenchymal finding. Mediastinal lymphadenopathy is often present, and may coalesce into large nodal masses (Wilde et al. 2005).

The principal initial treatment of PTLD is cessation or reduction of immunosuppression. However, PTLD may progress to an aggressive diffuse large B-cell lymphoma (Fig. 3). Only 50 % of pediatric lung transplant patients were reported to survive more than 2 years after diagnosis of PTLD in one study (Siegel et al. 2003), but that figure has likely improved in recent years.

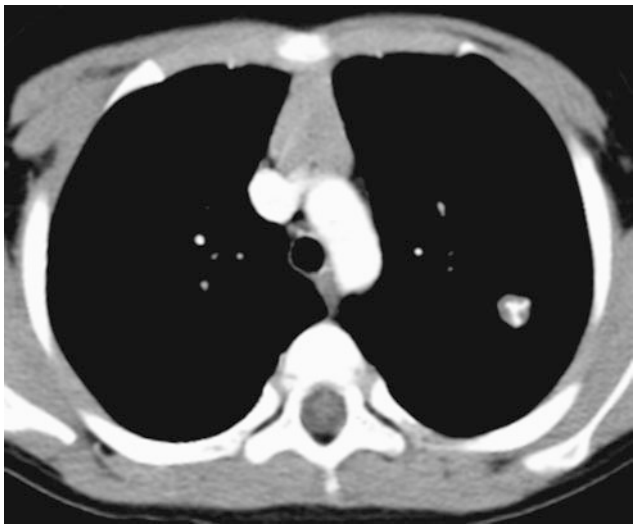

Fig. 4 Pulmonary hamartoma. Axial contrast-enhanced chest CT image shows a small, well-defined, lobular, left pulmonary nodule with curvilinear calcification

4.3 Pulmonary Hamartoma

Hamartomas account for the majority of benign tumors that occur in the lung parenchyma in childhood (Hancock et al. 1993). A pulmonary hamartoma consists of variable mesenchymal tissues that are native to the lung but present in an abnormal configuration. Despite being regarded as possible developmental anomalies, the vast majority of pulmonary hamartomas are discovered in adults and grow very slowly (doubling time longer than 550 days in almost all cases) (Huang et al. 2011), supporting the idea that hamartomas are actually acquired lesions.

Pulmonary hamartomas in adults are frequently asymptomatic and often found incidentally (Hartman and Shochat 1983). The characteristic radiological finding is a clearly defined solid nodular opacity in the lung periphery. Hamartomas measuring less than 1 cm in diameter are more likely to be spherical, and those measuring over 1 cm in diameter are more likely to be lobulated. Approximately 10 % show calcification, often with a speckled or curvilinear configuration (Fig. 4), and sometimes in a "popcorn" pattern. Central fat attenuation is seen in up to 30 % of hamartomas on CT. The likelihood of identifying fat or calcification increases with lesion size and these classic features are rarely seen in lesions measuring less than 2 cm in diameter. Hamartomas typically show no uptake on FDG-PET (Huang et al. 2011). MRI reveals linear or curvilinear clefts along the marginal surface, particularly on T2-weighted imaging. Most lesions demonstrate cleft and rim enhancement with contrast, but fat is usually inconspicuous on MRI (Park et al. 2008).

In contrast to adult patients, many of the reported cases of pulmonary hamartomas in younger children have fared poorly, including fatalities among those in the neonatal period (Hartman and Shochat 1983). Only a minority of the reported pediatric cases have been asymptomatic. Although pulmonary hamartomas typically manifest as isolated pulmonary nodules, these lesions may be quite large in young children.

Endobronchial hamartomas, which are particularly uncommon in childhood, present with respiratory symptoms or infections due to airway obstruction. A few reports of pediatric tracheal hamartomas exist, some of which may have a large extraluminal component manifesting clinically as a neck mass (Gross et al. 1996). Surgery for hamartomas is curative, although endobronchial hamartomas may require lobectomy or even pneumonectomy.

4.4 Pulmonary Chondroma

Pulmonary chondromas are benign lesions usually composed of myxoid rather than hyaline cartilage. The presence of a thin fibrous pseudocapsule, frequent bone metaplasia and calcification, and the absence of entrapped respiratory epithelium, smooth muscle, or fat allow distinction of pulmonary chondromas from hamartomas. On imaging, pulmonary chondromas appear as well-circumscribed nodules with or without calcification/ossification (Rodriguez et al. 2007). Pulmonary chondromas are the second most common component of the Carney triad, a rare nonfamilial disorder predominantly occurring in young women that also includes gastrointestinal stromal tumors (GISTs) and extraadrenal paragangliomas (Stratakis and Carney 2009) (Fig. 5). The chondromas associated with the Carney triad are usually asymptomatic and can be multiple (Rodriguez et al. 2007).

4.5 Fetal Lung Interstitial Tumor

Fetal lung interstitial tumor (FLIT) is a recently described, very rare tumor composed of immature interstitial mesenchyme in association with irregular airspace-like structures resembling the fetal lung at 20–24 weeks of gestation. In a case series of 10 patients, all presented by 3 months of age, and two were detected by prenatal ultrasound. Other than the two cases detected antenatally, all patients presented with respiratory distress (Dishop et al. 2010). One of the patients detected prenatally presented with a large pulmonary tumor causing fetal hydrops due to inferior vena cava obstruction

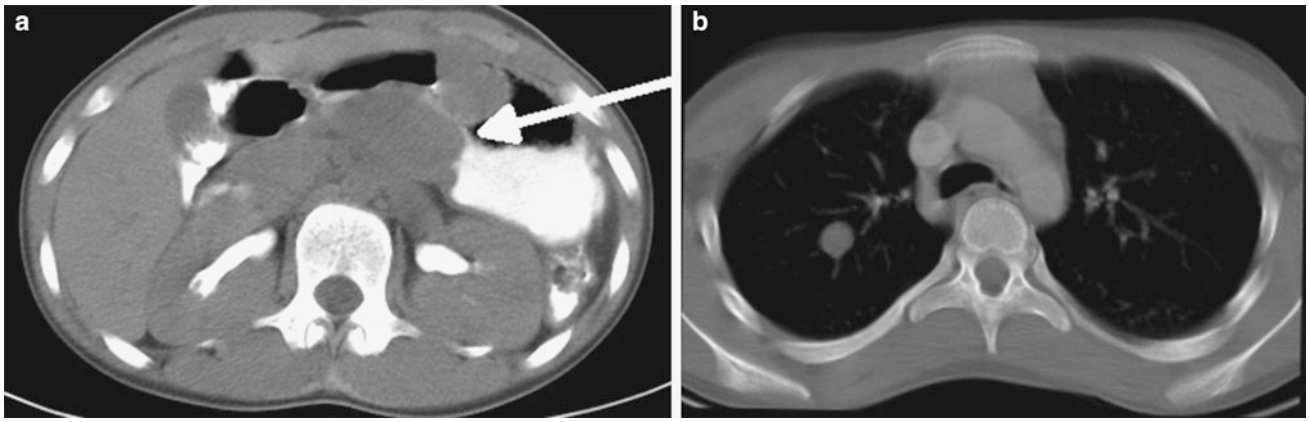

Fig. 5 Pulmonary chondroma. **a** Axial contrast-enhanced abdominal CT image in a 13-year-old female with incomplete Carney triad demonstrates a solid mass (*arrow*) along the distal wall of the stomach representing a gastrointestinal stromal tumor (GIST). **b** Axial chest CT image in the same patient shows a well-defined, solid right upper lobe pulmonary nodule without obvious calcification

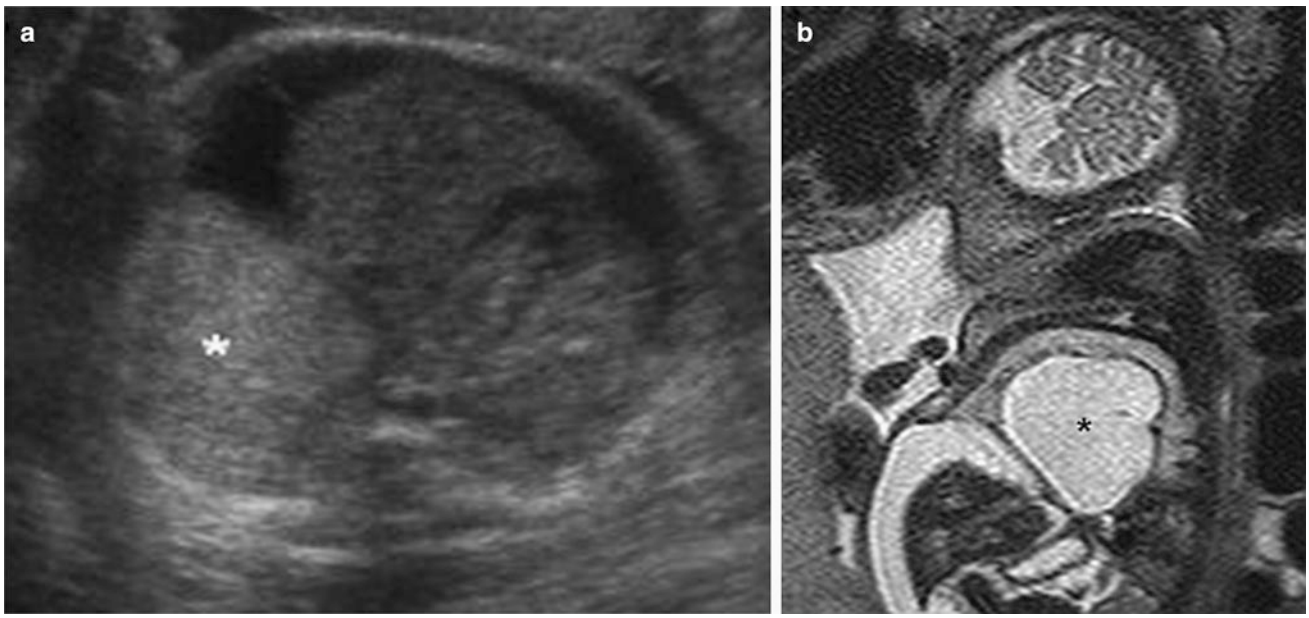

Fig. 6 Fetal lung interstitial tumor. **a** Transverse image from prenatal ultrasound exam performed at 36 weeks gestation reveals a large, well-circumscribed, solid hyperechoic right basilar lung mass (*asterisk*). **b** T2-weighted sagittal fetal MR image of the same patient demonstrates a large, well-circumscribed, high signal intensity mass (*asterisk*) compressing the adjacent lung and everting the diaphragm, with associated ascites related to inferior vena cava compression

and had ex utero intrapartum treatment (EXIT procedure) at 37 weeks gestational age (Lazar et al. 2011).

On imaging, these tumors are well-circumscribed, unifocal, and confined to a single lobe with a predilection for the right hemithorax. A majority are solid, although some may be partially cystic. They are homogeneously low in attenuation on CT imaging and the single case evaluated by MRI demonstrated heterogeneously increased signal intensity on T2-weighted images (Fig. 6). Prognosis is favorable, with no reports of malignant transformation or recurrence, even in incompletely resected cases (Dishop et al. 2010).

4.6 Infantile Myofibromatosis

Infantile myofibromatosis, the most common fibrous tumorous condition of infancy, most often presents with a firm nodular mass in the subcutaneous tissues. This entity, defined by a benign proliferation of fibroblasts and myofibroblasts, is subdivided into solitary and multicentric forms that may or may not have visceral involvement (Dishop and Kuruvilla 2008). The median age of presentation is 5 months for multicentric forms and 26 months for solitary forms (Levine et al. 2012). Myofibromas usually appear as a

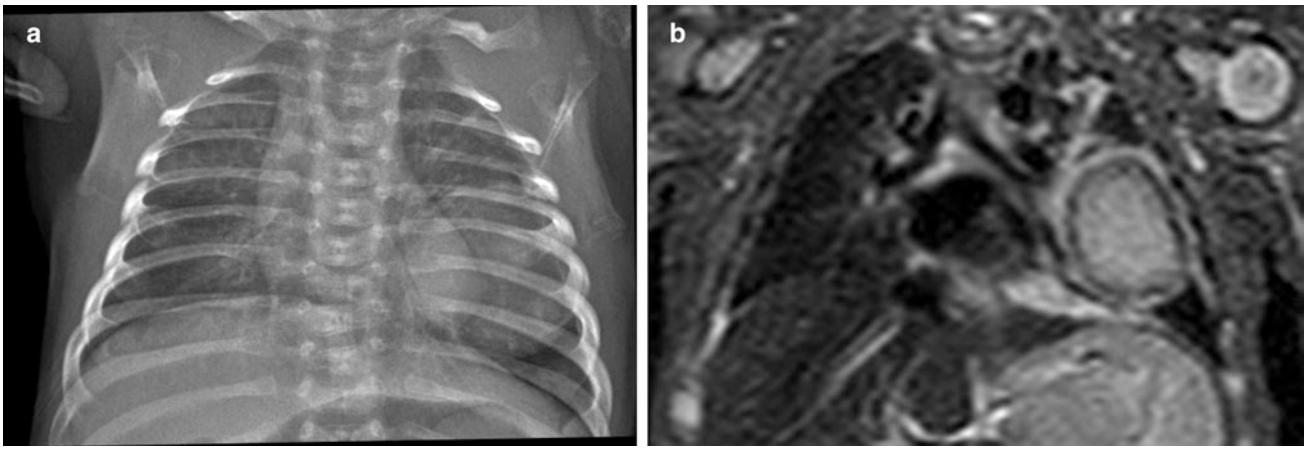

Fig. 7 Infantile myofibromatosis. **a** Frontal chest radiograph of a 1-month old shows a large, well-circumscribed mass of the left lower lung zone. **b** STIR coronal MR image of the same patient confirms the presence of a large left lung mass which exhibits central signal hyperintensity and a peripheral low signal intensity rim

mass with a thick-wall and a hypoechoic or anechoic center on ultrasound, and can demonstrate peripheral calcifications and adjacent bony erosion on CT. On MRI, they are usually hypointense on T1-weighted images and hyperintense with variable central hypointensity on T2-weighted images, and exhibit peripheral contrast enhancement (Koujok et al. 2005) (Fig. 7). Pulmonary masses may be a manifestation of multicentric visceral involvement and should not be misinterpreted as metastatic disease. Multicentric myofibromatosis with visceral involvement is associated with high morbidity and mortality despite chemotherapy and surgery, while the prognosis is excellent in other forms with surgery alone (Levine et al. 2012).

4.7 Congenital Peribronchial Myofibroblastic Tumor

Congenital peribronchial myofibroblastic tumor (CPMT) is a very rare tumor that is thought to develop at approximately 12 weeks of gestational age and demonstrates variable degrees of smooth muscle and cartilaginous differentiation (Alobeid et al. 1997). The tumor is typically detected in the neonatal period, and antenatal presentation with fetal hydrops has been reported (Horikoshi et al. 2005). Although histologically benign, CPMT can exhibit certain aggressive features such as frequent mitoses, necrosis, and infiltrative growth, leading some cases to be reported as malignant entities such as bronchopulmonary fibrosarcoma (Kim et al. 2013). No syndromic, genetic, or maternal associations have been identified (Travis et al. 2004).

On imaging, CPMT typically appears as a large, single well-circumscribed pulmonary mass without lobar predilection. The tumors typically measure 5–7 cm in diameter and occupy the majority of the involved hemithorax, exerting mass affect with mediastinal shift (Travis et al. 2004). Hydrops fetalis is reported in 36 % and polyhydramnios in 27 % of cases (Horikoshi et al. 2005). CPMT has a heterogeneously hyperechoic appearance on ultrasound and a heterogeneous appearance on CT without cysts or calcifications (Travis et al. 2004). The appearance on MRI has not been described.

Patients generally survive CPMT following complete surgical resection. However, some die in the prenatal or neonatal period as a result of hydrops fetalis or respiratory failure (Huppmann et al. 2011). No local recurrence or metastasis of CPMT has been reported.

4.8 Inflammatory Myofibroblastic Tumor

Inflammatory myofibroblastic tumor (IMT) is a borderline or low-grade malignancy that can occur at a variety of sites, with the lungs being second only to the abdomen. Previously known as inflammatory pseudotumor or plasma cell granuloma, the current nomenclature emphasizes the dominant component of spindle cells, accompanied by variable numbers of inflammatory cells, particularly eosinophils, lymphocytes, and plasma cells (Yousem et al. 2004).

The important function of the myofibroblast in tissue repair is consistent with the hypothesis that an aberrant response to tissue injury underlies the pathogenesis of these lesions. A variety of unusual microorganisms have been implicated in individual case reports, including *Mycobacterium avium intra-cellulare*, *Corynebacterium equi*, *Coxiella burnetii*, and *Bacillus sphaericus* (Hedlund et al. 1999). More recently, viruses such as EBV and HHV-8 have also been implicated (Mergan et al. 2005).

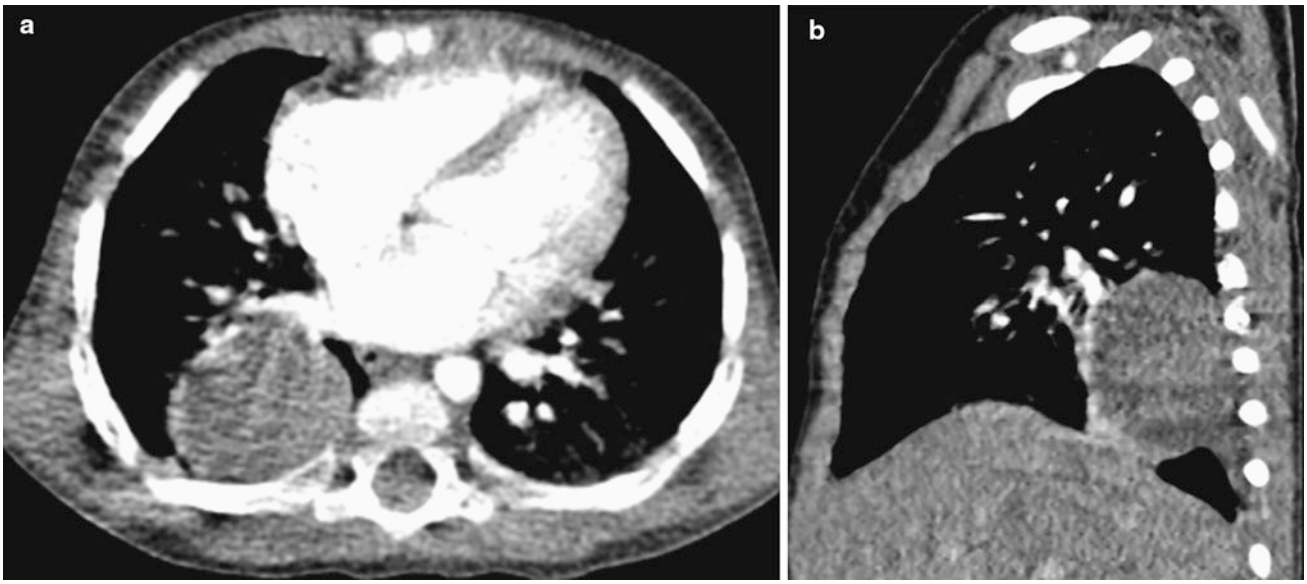

Fig. 8 Inflammatory myofibroblastic tumor (IMT). **a** Axial contrast-enhanced chest CT image in a 13-month-old girl who had intermittent unexplained fever. A chest radiograph had shown a rounded right lower lobe mass, confirmed to be solid on CT. **b** Sagittal contrast-enhanced CT image shows pleural extension of the mass posteroinferiorly, but no associated pleural effusion or chest wall invasion

IMT has been reported to account for 14 % of primary lung tumors, a similar proportion to tumors such as pleuropulmonary blastoma and bronchial carcinoid (Hancock et al. 1993). The mean age of presentation is 13 years. Although pulmonary IMT can be asymptomatic, it can also present with cough, chest pain, or a constellation of fever, weight loss, anemia, thrombocytosis, polyclonal hyperglobulinemia, and elevated inflammatory markers (Coffin et al. 2007). An association with hypertrophic pulmonary osteoarthropathy has been reported (Mas Estelles et al. 1995).

The typical imaging appearance of IMT is a well-circumscribed, solitary, upper lobe predominant pulmonary mass, with a mean size of 8.4 cm (Coffin et al. 2007; Siminovich et al. 2012). About 80–85 % is parenchymal, with the remainder being endobronchial (Hancock et al. 1993) (Fig. 8). IMTs typically are low in attenuation on noncontrast CT imaging with slight enhancement on early phase post-contrast imaging and heterogeneous enhancement on delayed phase post-contrast imaging, although single phase contrast-enhanced CT scanning should generally suffice for lesion evaluation (McHugh and Disini 2011). Calcification or cavitation is rarely seen. On MRI, IMTs typically demonstrate homogeneous slightly low signal intensity on T1-weighted images, variable hyperintensity on T2-weighted images, and heterogeneous contrast enhancement that is most pronounced in the delayed phase (Takayama et al. 2008). Hilar lymphadenopathy and pleural effusion are not commonly associated (Mas Estelles et al. 1995). Although bronchi and vessels may be trapped within the pulmonary masses and become narrowed distally or even obliterated, atelectasis is observed in only 14 % of pediatric patients (Verbeke et al. 1999).

Locally aggressive IMTs are occasionally seen and may invade the mediastinum, chest wall, or diaphragm (Hedlund et al. 1999; Verbeke et al. 1999; Yousem et al. 2004). CT and MRI are both useful in characterizing the extent of these aggressive lesions in relation to the airways, esophagus, cardiovascular structures, and chest wall (Hedlund et al. 1999). Lesions arising solely in the esophagus have been described, and barium esophagography can be useful for characterizing esophageal involvement when suspected.

Over-expression of the ALK1 (anaplastic lymphoma kinase) gene is associated with an increased rate of local recurrence but not distant metastases, and an overall improved prognosis. Recurrent and metastatic IMTs tend to be larger (Coffin et al. 2007). Many IMTs act in a relatively indolent fashion, although about one-quarter recur. Pulmonary resection with removal of all gross evidence of disease is the mainstay of treatment and is usually curative for tumors confined to the lung. Locally aggressive lesions may require more radical surgery including pneumonectomy rather than the more usual segmental or lobar resection. When these tumors extend beyond the organ of origin at diagnosis, up to 46 % relapse locally (Janik et al. 2003). Relapse or invasion of the mediastinum has occasionally been treated with immunosuppressive therapy or even multiagent chemotherapy with good results (Verbeke et al. 1999; Janik et al. 2003). Metastases have been documented to the lung, liver, bone, and brain (Coffin et al. 2007; Siminovich et al. 2012).

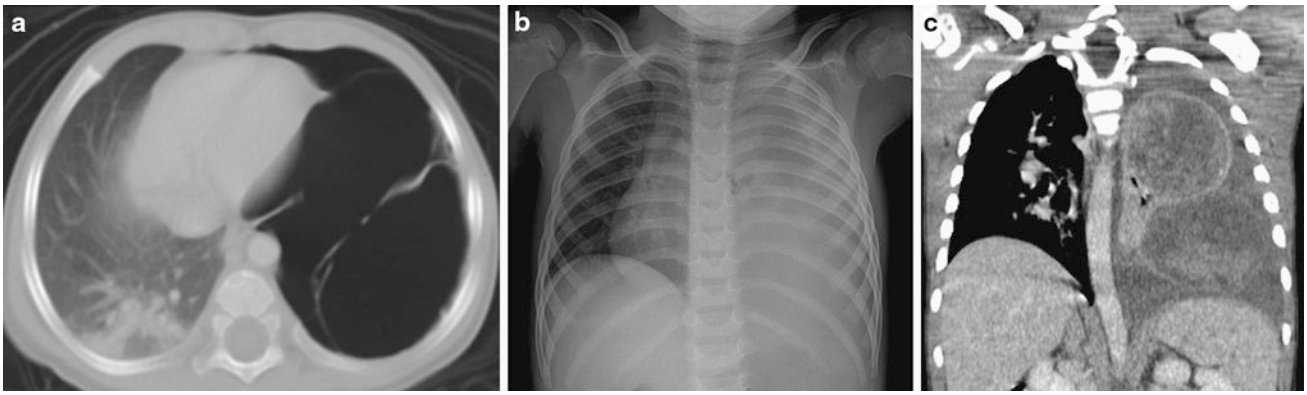

Fig. 9 Pleuropulmonary blastoma (PPB). **a** Axial chest CT image from a 1-year old with a history of spontaneous pneumothorax demonstrates a large, thin-walled, septated, air-filled, cystic lesion of the left lung representing a Type I (cystic) PPB. **b** Frontal chest radiograph of a different patient at 3 years of age shows near complete opacification of the left hemithorax with rightward mediastinal shift, findings evocative of complicated pneumonia with empyema. **c** Coronal contrast-enhanced chest CT image reveals a bilobed heterogeneously enhancing mass arising from the left lung representing a Type III (solid PPB), with an associated left pleural effusion

4.9 Pleuropulmonary Blastoma

Although previous reports report a similar incidence to IMTs and bronchial carcinoids (Hancock et al. 1993), pleuropulmonary blastoma (PPB) is likely the most common primary lung malignancy of childhood (Priest et al. 1997). The mean age at presentation is 38 months, and it is rarely seen in children over 6 years of age. Prenatal presentation has also been reported (Miniati et al. 2006). Approximately 30–40 % of PPB patients or their relatives have manifestations of the PPB Family Tumor Dysplasia Syndrome (PPB-FTDS), an autosomal dominant genetic disorder with a distinctive predisposition to certain tumors and dysplasias, including PPB, cystic nephroma, multinodular goiter, Sertoli-Leydig cell tumor, cervical embryonal rhabdomyosarcoma, pituitary blastoma, pineoblastoma, nasal chondromesenchymal hamartoma, and ciliary body medulloepithelioma (Slade et al. 2010; Foulkes et al. 2011). Approximately 70–75 % of patients with PPB have germline mutations in the DICER1 gene that encodes a protein involved in microRNA processing (Priest 2012).

PPB is composed of a malignant mesenchymal component resembling fetal lung in early gestation with a variably sarcomatous or blastematous appearance, but no malignant epithelial component. Rhabdomyosarcomatous areas in PPB are identical to embryonal rhabdomyosarcoma, and cases of PPB have been misdiagnosed as rhabdomyosarcomas arising in a congenital cystic adenomatoid malformation (CCAM) (Pai et al. 2007) or in normal lung (Schiavetti et al. 2009). Recognition of high grade blastemal elements, cartilage, spindle cell sarcoma, or diffuse-marked anaplasia facilitates the correct diagnosis of PPB in a pediatric lung mass. PPB is distinct from pulmonary blastoma, a biphasic sarcomatoid carcinoma predominantly occurring in adults (Dehner 1994).

Three subtypes of PPB are described based on gross morphology. Type I is a unilocular or multilocular cyst with delicate fibrous septa, Type II PPB is mixed cystic and solid and Type III PPB is entirely solid (Dehner et al. 1995; Priest et al. 2006). There is a significant difference in the age at presentation. The median age at diagnosis is 10 months for type I, 34 months for type II, and 44 months for type III (Priest et al. 2006). Progression of unresected Type I PPB to Type II and III PPB can occur. Type I PPB may also spontaneously regress, whereby it is classified as Type I-regressed PPB (Type Ir PPB). Types I and Ir PPB are indistinguishable on gross inspection from the large-cyst form of CCAM; however, CCAMs do not transform into PPBs (Priest et al. 2009).

The clinical presentation of PPB is varied and nonspecific, ranging from incidental detection to cough, chest pain, and respiratory distress. Type I and Ir PPBs appear as well-defined, air-filled cysts confined to the lung parenchyma or visceral pleura, and the presence of multifocal cysts or spontaneous pneumothorax favors type I PPB over large-cyst CCAM (Priest et al. 2009). Type II and III PPBs typically manifest as a large mass in the hemithorax, often in the lung periphery adjacent to the pleura, with associated mediastinal mass effect and pleural effusion (Priest et al. 2006) (Fig. 9). Invasion of the chest wall or diaphragm is occasionally observed. Local invasion of the bronchi, great vessels, and heart is rare (Goel et al. 2010; Priest et al. 2011). The solid components of the mass demonstrate contrast enhancement on CT and MRI. Some type II and III PPBs are sharply demarcated from adjacent lung parenchyma while others may be more infiltrative. Confident assignment of the site of origin is often difficult to determine with large lesions.

Initial misdiagnosis is common, with Type I PPBs mimicking large-cyst CCAMs, and type II and III PPBs

mimicking other tumors or complicated pneumonia with empyema. These tumors are so friable intraoperatively that empyema may still be suspected during surgery (Buyukavci et al. 2006). The diagnosis depends on histological evaluation that in most cases takes place after attempted or successful surgical resection. The malignant elements in Type I PPBs can be very subtle, requiring meticulous inspection of the pathology specimen to make the correct diagnosis.

Type I PPBs have a better prognosis than the other subtypes. Local recurrence is unusual in Type I PPB, occurring in fewer than 15 %, but develops in more than 45 % of Types II and III. Metastases occur in 11 % of Type II and 55 % of Type III cases (Priest 2012). Metastases have a particular tropism for the central nervous system including the spinal cord (Priest et al. 1997), so that craniospinal MRI is merited at staging and follow-up. The second most common site for metastatic spread is the skeletal system. Metastases to the liver, adrenals, and ovary are also reported (Priest 2012). The use of adjuvant chemotherapy in addition to surgery confers a survival advantage for all three subtypes (Priest et al. 2006). Overall survival is 90 % for Type I and 40–60 % for Types II and III (Priest 2012). Extrapulmonary involvement and incomplete resection confer a worse prognosis (Indolfi et al. 2007).

4.10 Bronchial Carcinoid Tumor

Bronchial carcinoid tumors arise from neuroendocrine Kulchitsky cells in the airways. Although bronchial carcinoid is the most common malignant endobronchial tumor and the second most common primary pediatric malignancy of the lower respiratory tract (Dishop and Kuruvilla 2008), it is still uncommon in children relative to adults. When it occurs in children, it tends to present in adolescents (Al-Qahtani et al. 2003). The actual carcinoid syndrome is very rare in childhood outside the setting of metastatic disease (Hancock et al. 1993). Cushing syndrome from ectopic adrenocorticotropic hormone secretion has also been described but is similarly uncommon (Wang et al. 1993). Children with bronchial carcinoids are much more likely than their adult counterparts to present with post-obstructive wheezing and atelectasis, in addition to hemoptysis and pneumonitis (Wang et al. 1993). A carcinoid in an asymptomatic patient is more likely to involve a peripheral airway than a central airway (Curtis et al. 1998). Bronchial carcinoids usually have intraluminal, mural, and extrabronchial components. Up to 4 % of carcinoid tumors are associated with other endocrine neoplasias, the most common association being with pituitary tumors (Al-Qahtani et al. 2003).

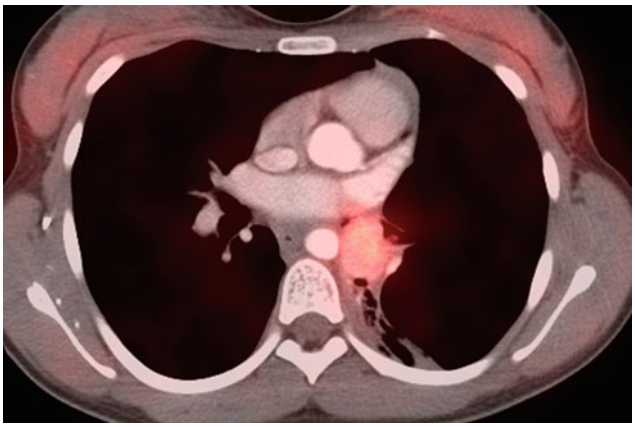

Fig. 10 Bronchial carcinoid tumor. A fused axial chest image from an In-111 octreotide SPECT-CT scan in a 12-year old shows avid radiopharmaceutical uptake by a hyper-enhancing soft-tissue mass along the distal left mainstem bronchus

The majority of carcinoid tumors are not visible on CXR and their true extent may be difficult to determine even on high-resolution CT. The typical CT appearance is of a single round or lobulated mass that is at least partially endobronchial (Jeung et al. 2002). They are hypervascular polypoid tumors and characteristically show prominent contrast enhancement. Occasionally, the mass external to the bronchus is larger than that in the lumen, and the extrabronchial component may consequently be visible as a hilar mass. The mass resides along the main, lobar, or segmental bronchi in 80 % of cases, with a predilection for branching sites. The mass involves the more peripheral airways in the other 20 % of cases (Chong et al. 2006). Approximately one quarter of carcinoid tumors in adult patients are calcified, but the frequency of calcification is much less in childhood. Bronchial carcinoids typically demonstrate hyperintensity on T2-weighted images and avid homogeneous contrast enhancement on MRI. Bronchial carcinoids show increased octreotide uptake on somatostatin receptor scintigraphy in greater than 85 % of cases (Jeung et al. 2002) (Fig. 10). Although not yet widely available, the novel PET tracers 68-Ga-DOTATOC and 18F-DOPA in combination with integrated CT offer higher spatial resolution than conventional somatostatin scintigraphy and improved sensitivity for the detection of carcinoid tumor (Koopmans et al. 2008; Buchmann et al. 2007). The incidence of metastases with bronchial carcinoids in children is 10–15 % (Wang et al. 1993). Metastases are most commonly seen in the liver, adrenals, brain, and bone. Pediatric bronchial carcinoids generally have an excellent prognosis with complete resection and lymph node excision. Recurrence has been reported in as many as 20 % of cases but usually can be successfully treated surgically (Rizzardi et al. 2009).

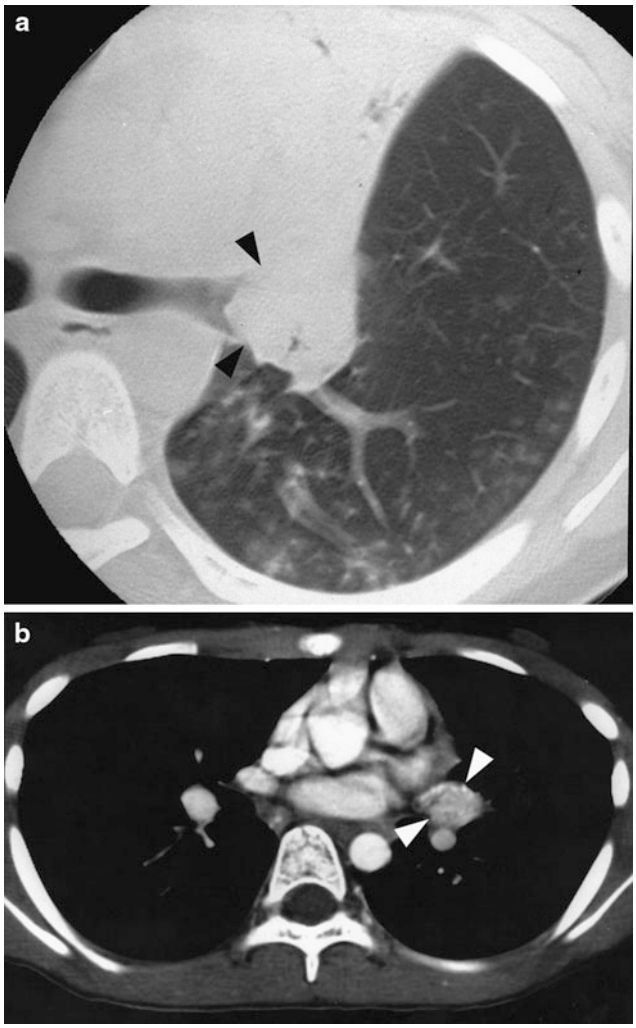

Fig. 11 Mucoepidermoid carcinoma. **a** Axial chest CT image showing an endobronchial mass (*arrowheads*) nearly occluding the left mainstem bronchus close to the origin of the upper lobe bronchus with associated upper lobe collapse. **b** Axial contrast-enhanced chest CT image from a different patient demonstrating an enhancing, hypervascular mass (*arrowheads*) at the origin of the lingular bronchus (Courtesy of Dr. H. Hara, Tokyo)

4.11 Mucoepidermoid Carcinoma

Mucoepidermoid carcinoma, the second most common pediatric endobronchial malignancy (Al-Qahtani et al. 2003), is thought to originate from the minor salivary glands lining the airways. Mucoepidermoid carcinoma is graded by histology similar to other salivary-type neoplasms into low, intermediate, and high grades. Pediatric mucoepidermoid carcinomas are generally low grade, low stage lesions (Andronikou and Kader 2001).

As with other endobronchial lesions, the history is usually that of respiratory infections or lobar collapse with or without air trapping. Up to 25 % of patients are asymptomatic (Al-Qahtani et al. 2003). The typical imaging appearance is of a single round, lobulated, or polypoid mass in a lobar bronchus (Kim et al. 1999). Calcification is seen in 50 % of tumors. Contrast enhancement may be marked, suggesting hypervascularity (Fig. 11). Although endoscopy remains the diagnostic procedure of choice for endobronchial lesions, their "tip-of-the-iceberg" endobronchial nature makes endoscopic resection inadvisable. Grades are indistinguishable by imaging. Lymphadenopathy and distal metastasis are unusual, being seen in less than 10 % of cases (Wu et al. 2011). Thoracotomy, with lymph node sampling, is the recommended treatment to ensure histologically negative margins (Morini et al. 2003). For low-grade tumors without lymph node metastases, complete resection should result in a good outcome (Xi et al. 2012).

4.12 NUT Midline Carcinoma

NUT midline carcinoma is a poorly differentiated aggressive carcinoma associated with characteristic rearrangement of the nuclear protein in testes (NUT) promoter gene. The largest published series of NUT midline carcinomas to date consisted of 22 cases (French 2010). No clear gender predilection is evident, and the mean age of diagnosis is 25 years. The presenting symptoms vary depending on the primary site of tumor or the presence of metastases.

NUT carcinomas arise in the mediastinum, upper aerodigestive tract, neck, or head in the majority of cases (French 2010). Other reported primary sites include the salivary glands, liver, bladder, pelvic skeleton, and extremity soft tissues (French et al. 2004; den Bakker et al. 2009). Pulmonary cases may originate from basal cells of the bronchiolar epithelium (Tanaka et al. 2012). A midline location is noted in 70 % of cases (Polsani et al. 2012). Apart from the midline location, imaging features are nonspecific. A heterogeneous low attenuation mass with central areas of necrosis has been reported on CT with occasional small central calcifications. On MRI, the mass exhibits decreased signal intensity on T1-weighted images, mildly increased signal intensity on T2-weighted images, and heterogeneous contrast enhancement. Both the primary tumor and metastases are FDG-avid on PET (Rosenbaum et al. 2012). The lungs are the most common site of metastases and metastases to the liver, kidney, brain, spinal cord, and subcutaneous soft tissues have also been reported (Polsani et al. 2012).

Intrathoracic NUT carcinomas have a poor prognosis. Widespread metastases are typically present at diagnosis, and intrathoracic growth produces superior vena cava compression. A mean survival of 9.5 months is reported (French 2010).

4.13 Papillomas and Squamous Cell Carcinoma

Papillomas are the most common benign tumor of the lower respiratory tract in children (Dishop and Kuruvilla 2008). Recurrent respiratory papillomatosis (RRP) is primarily caused by vertical transmission of human papillomavirus (HPV), most frequently HPV types 6 and 11 (Cook et al. 2000). Childhood RRP has a bimodal peak of 2 and 10 years of age and no sex predilection has been established (Rabah et al. 2001). Although usually isolated to the larynx, papillomas develop in the lower airways in up to 8 % of RRP cases, with lung parenchymal nodules occurring in approximately 1 % of cases (Soldatski et al. 2005). The occurrence of lower airway and pulmonary lesions may be exacerbated by treatment of the primary laryngeal lesions, including tracheostomy for tracheal stenosis and recurrent intubation. It is hypothesized that detached fragments are carried down the airways during inspiration and can enlarge if not expelled by mucociliary clearance (Kramer et al. 1985).

Airway papillomas may be localized or extensive. Conglomerate lesions typically manifest as endotracheal or endobronchial masses. Papillomas have a classic fimbriated or "salmon egg" appearance on endoscopy. They are predominantly endoluminal, although submucosal infiltration does occur with more extensive papillomas. Pulmonary parenchymal lesions typically have a nodular appearance and may be widely scattered remote from the major bronchi. The nodules may be thin or thick walled and may cavitate (Fig. 12). Air-fluid levels can be seen with superimposed hemorrhage or infection. Some lesions occasionally resemble dilated bronchi or bronchiectasis but close inspection shows no direct communication to more central bronchi (Williams et al. 1994). An intraluminal airway mass with concomitant pulmonary nodules or cavities is highly suggestive of laryngotracheal papillomatosis.

Children with RRP may present with cough and fever due to atelectasis, consolidation, and bronchiectasis related to airways obstruction and recurrent superinfection (Williams et al. 1994). RRP associated with HPV 11 has a more aggressive course and worse prognosis than RRP associated with HPV 6 (Rabah et al. 2001). Severe lung damage from multiple destructive parenchymal lesions may result in symptoms of restrictive lung disease in addition to upper airway obstruction. Malignant transformation into squamous cell carcinoma is another potential complication of RRP (Katz et al. 2005), and is associated with HPV 11 (Cook et al. 2000). Benign papillomas can demonstrate increased FDG uptake on PET and be confused with malignancy (Pipavath et al. 2008). Interval lesion growth,

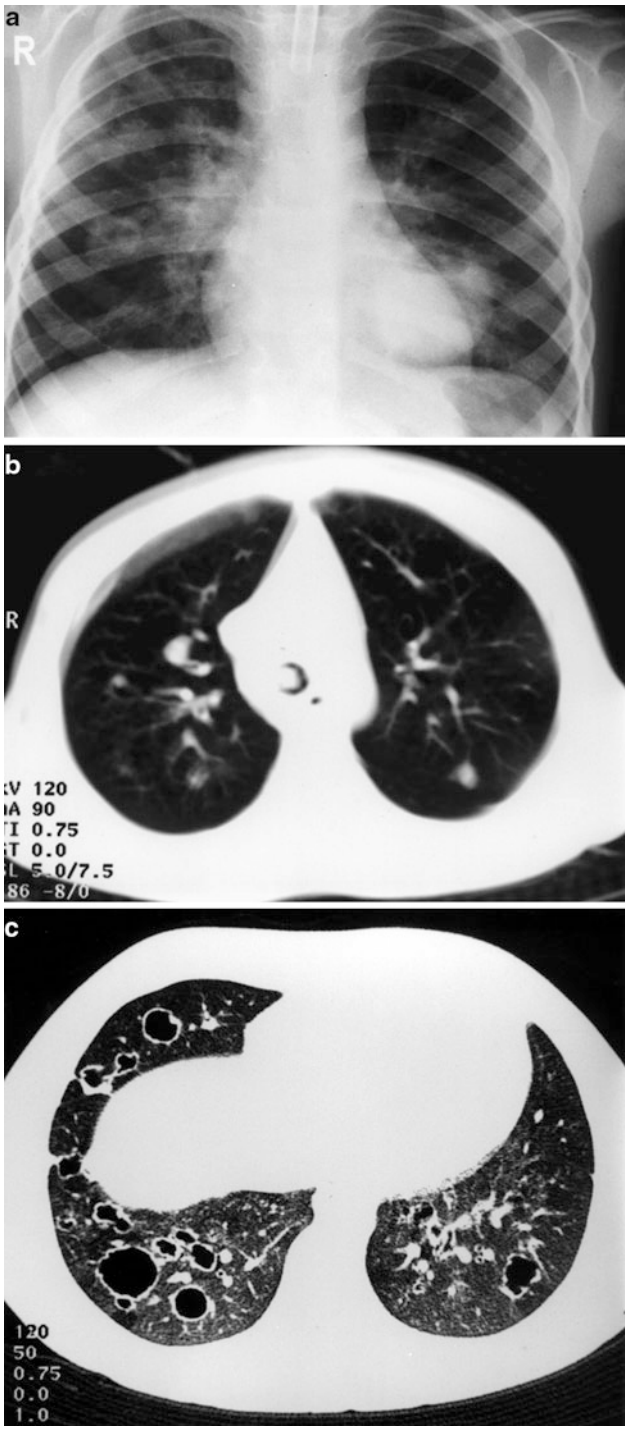

Fig. 12 Recurrent respiratory papillomatosis (RRP) with lung involvement. **a** Frontal upright chest radiograph showing two cavitary lung nodules, with an air-fluid level in the larger, left-sided lesion. **b** Axial chest CT image demonstrating an endotracheal mass and bilateral pulmonary nodules. **c** Numerous bilateral cavitary pulmonary nodules of varying sizes, many with thick, irregular walls

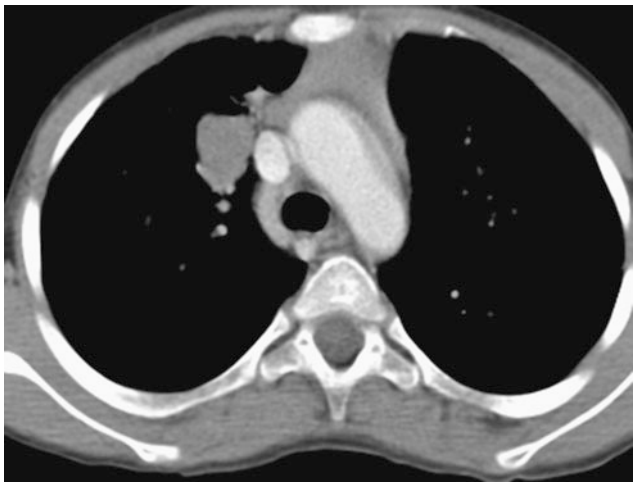

Fig. 13 Leiomyoma. Axial contrast-enhanced chest CT image from an HIV + 11-year old shows a lobular solid mass of the medial right upper lobe

increasing lesion wall thickening, thoracic lymphadenopathy, and the presence of metastases are findings that suggest malignant transformation.

4.14 Leiomyoma and Leiomyosarcoma

Leiomyoma and leiomyosarcoma of the pediatric lower respiratory tract are very rare and reside along a spectrum of benign to malignant tumors of smooth muscle origin. There is an association between smooth muscle tumors, immunosuppression related to solid organ transplantation or human immunodeficiency virus (HIV) infection (Chadwick et al. 1990), and Epstein–Barr virus (EBV) expression within the tumor cells (McClain et al. 1995). Clonality studies indicate that multifocality of these lesions is often caused by infection of multiple cells rather than metastasis (Parham et al. 2012).

Patients with smooth muscle tumors of the lower respiratory tract usually present with nonspecific respiratory signs and symptoms (Lal et al. 2005). Since most affected patients are immunosuppressed, infection is often the initial concern, leading to a delay in diagnosis (McClain et al. 1995). Although the majority of smooth muscle tumors of the respiratory tract are found in the lung parenchyma and less than one-third of cases manifest as endobronchial lesions, they are thought to arise from smooth muscle of the bronchi or bronchioles. They typically present as single or multiple well-defined solid pulmonary masses (Balsam and Segal 1992) (Fig. 13). The tumor behavior is usually indolent, and treatment consists of some combination of surgery, chemotherapy, and reduction of immunosuppression (Parham et al. 2012).

5 Extrathymic Mediastinal Tumors

Lymphoma, leukemia, and primary neoplasms of the thymus are covered in the chapter entitled Imaging Evaluation of the Thymus and Thymic disorders in Children by Sams and Voss in this book. Hemangiomas, vascular malformations, and neurofibromas are addressed in the chapter entitled Radiology of the Chest Wall by Eich, Kellenberger, and Willi.

5.1 Germ Cell Tumors

Primary germ cell tumors (GCT) account for up to 10 % of all mediastinal masses in children and are second only to lymphoma as a cause of an anterior mediastinal mass. (Dulmet et al. 1993). Only 2–3 % of mediastinal GCTs occur in the posterior mediastinum. An intrapulmonary location is exceedingly rare. There is an association among nonseminomatous mediastinal germ cell tumors, hematological malignancies, and Kleinfelter syndrome (XXY) (Strollo et al. 1997).

Up to 50 % of affected patients have no symptoms at the time of diagnosis (Sasaka et al. 1998). Large tumors may cause tracheal compression, superior vena cava obstruction, or fetal hydrops. Occasionally, ectopic production of sex hormones or insulin leads to presentation with pseudoprecocious puberty or hypoglycemia before the onset of respiratory symptoms. GCTs, which include teratomas, teratocarcinomas, seminomas, dysgerminomas, embryonal cell carcinomas, endodermal sinus tumors, and choriocarcinomas, usually do not present before the second decade of life, but can be detected by prenatal ultrasound. GCTs are malignant in about 10 % of cases. Malignant GCTs have a male predilection and are frequently associated with elevated serum levels of human chorionic gonadotropin or alpha-fetoprotein. Teratomas account for the vast majority of mediastinal GCTs in children and have varied amounts of mature and immature somatic tissues. Mature teratomas are benign lesions composed of well-differentiated ectodermal, mesodermal, and endodermal derivatives, and are curable by surgical resection. Immature teratomas are potentially malignant but in patients less than 15 years of age have biological and clinical behavior similar to mature teratomas (Dulmet et al. 1993). The prognosis for other malignant mediastinal GCTs in childhood is poor (Yalcin et al. 2012).

CT attenuation values and MR signal intensity for these tumors are highly variable depending on the amount of fat, calcium, fluid, or soft tissue in the mass. Most teratomas have well-defined margins, thick walls, and some fatty tissue and/or calcification (Alper et al. 2005) (Fig. 14). Fatty tissue plus calcification in an anterior mediastinal mass almost invariably indicate a germ cell origin. Seminomas

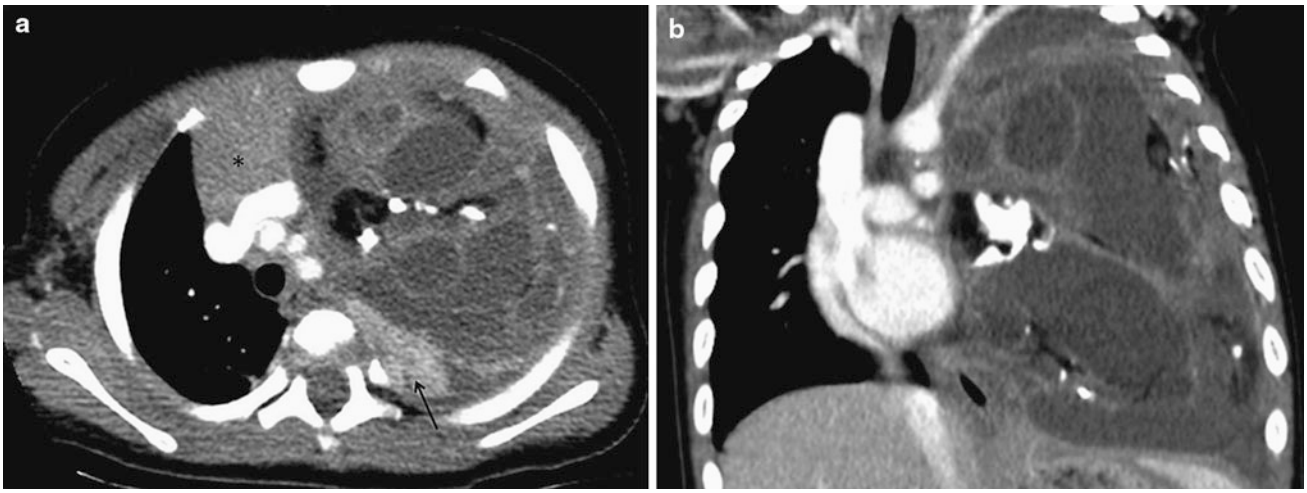

Fig. 14 Teratoma. **a** Axial contrast-enhanced chest CT image in a 15-month-old girl, who presented with cough and respiratory distress, shows a mixed cystic and solid mass that contains calcific and fatty elements. The mass appears to be separate from the displaced thymus (*asterisk*), and left lower lobe compressive atelectasis (*arrow*) is also evident. **b** A coronal contrast-enhanced chest CT image shows mediastinal displacement by the mass and close proximity of the mass to the heart, but no pericardial effusion. There is no tracheal compression despite the tracheal displacement

typically have more homogeneous, soft-tissue attenuation. Features suggesting malignancy include large size, ill-defined margins, and extensive central necrosis, but there is wide variation in the appearance of these tumors (Strollo et al. 1997).

Teratomas may rupture into adjacent structures such as the pleural space, pericardium, airways, or pulmonary air spaces. Up to one-third of mature benign mediastinal teratomas are reported to rupture, with malignant lesions having a lesser tendency to leak their contents (Sasaka et al. 1998). Severe symptoms such as chest pain or hemoptysis are more commonly found in ruptured than in unruptured tumors (Choi et al. 1998). Proteolytic or digestive enzymes and sebaceous materials within these teratomas are thought to play a role in their tendency to rupture and incite adjacent inflammation. High amylase levels have been found in pleural effusions and in the tumor contents (Sasaka et al. 1998). Ruptured tumors tend to display more heterogeneity in their internal components than unruptured teratomas. Ancillary findings in ruptured tumors depend on the space into which the rupture occurs. Rupture into an airway or lung may cause a chemical pneumonitis or fat-containing masses in the adjacent lung parenchyma. Hemoptysis with expectoration of hair or sebaceous material indicates a fistula between the tumor and the airway (Sasaka et al. 1998; Alper et al. 2005). Rupture into the pleura or pericardium results in pleural or pericardial effusions (Choi et al. 1998). Rupture is important to recognize as inflammation and adhesions secondary to extravasation of tumor contents may result in more hazardous and extensive surgery than had been anticipated.

5.2 Neuroblastic Tumors

The majority of posterior mediastinal masses in children are neurogenic tumors arising from the paravertebral sympathetic chain. The major childhood neurogenic tumors are neurofibromas, neuroblastoma, ganglioneuroblastoma, and ganglioneuroma. Neuroblastoma and ganglioneuroblastoma occur in the first decade of life whereas the benign ganglioneuroma, in which all cells are mature, is typically seen in older children and adolescents.

Thoracic neuroblastoma accounts for 15 % of all cases of neuroblastoma and typically has a better outcome than primary abdominal neuroblastoma. In one series of 96 children with thoracic neuroblastoma, the median age at presentation was at 0.9 years, only 20 % had metastatic disease, and actuarial survival was 88 % at 4 years (Adams et al. 1993). In this series, a posterior mediastinal mass was diagnosed incidentally on chest radiographs performed for non-tumor-related symptoms in half the cases.

In most instances, the diagnosis of a neuroblastic tumor is suggested by CXR findings, particularly when posterior rib erosion is seen indicating a posterior mediastinal mass. On CT, most thoracic neuroblastic tumors are well-circumscribed, fusiform masses oriented in a paraspinal location. Approximately 40 % contain some calcification. Only about 2 % of primary thoracic neuroblastomas will have pulmonary metastases visible at diagnosis (DuBois et al. 2008). MRI demonstrates hypointensity on T1-weighted images and variable intermediate or high signal intensity on T2-weighted images, with signal voids corresponding to calcifications or

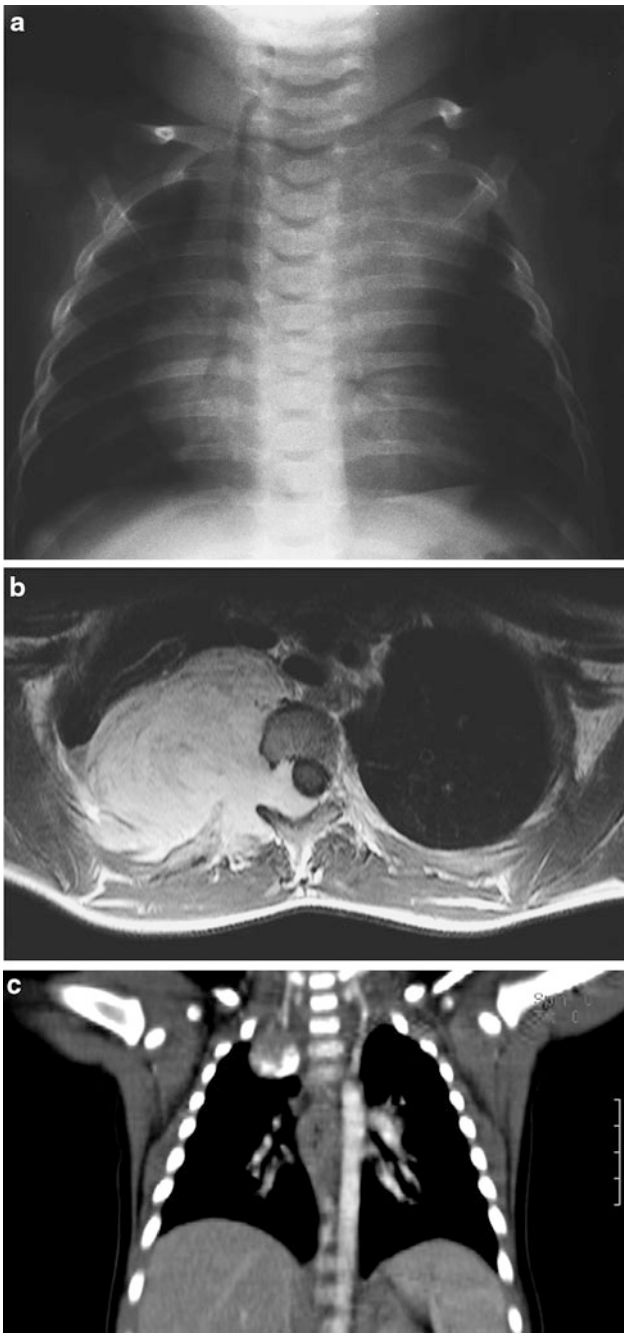

Fig. 15 Neuroblastoma. **a** Frontal chest radiograph of an infant showing an opacity in the left upper hemithorax and posterior rib erosion indicative of a posterior mediastinal mass. **b** Axial contrast-enhanced T1-weighted chest MR image from a different patient demonstrates a large right-sided mass lesion with intraspinal and posterior chest wall invasion. **c** A coronal contrast-enhanced chest CT image from a different 6-month-old patient shows a calcified mass of the right apical hemithorax

encased vessels (Fig. 15). Non-necrotic portions of neuroblastic tumors demonstrate avid contrast enhancement (Daldrup et al. 1997).

The International Neuroblastoma Risk Group (INRG) Project has proposed the new INRG Staging System (INRGSS) that shifts the focus from surgicopathologic to imaging findings for neuroblastic tumors. The INRGSS system includes two stages of localized disease that are dependent on whether or not image-defined risk factors (IDRFs) are present at the time of diagnosis (Brisse et al. 2011). Stage L1 tumors are localized tumors that do not involve vital structures, as defined according to the IDRFs, and stage L2 tumors are local–regional tumors with one or more IDRFs. IDRFs in the chest relate to vascular encasement, airway compression, or neural encroachment (Table 2).

There is no current consensus regarding the optimal imaging modality for assessment of local–regional disease in neuroblastic tumors. Although MRI has long been recognized as an effective method for imaging neuroblastoma and provides excellent visualization of the intraspinal contents, superiority of MRI over CT for local–regional staging has not been demonstrated (Siegel et al. 2002). Metaiodobenzylguanidine (MIBG) scintigraphy should be routinely performed to identify metastatic disease, ideally with single photon emission computed tomography (SPECT) or SPECT-CT to allow better identification and localization of small foci of uptake that are difficult to see on planar MIBG scans (Brisse et al. 2011). The role of whole-body MRI and PET in neuroblastic tumors is not yet clearly established.

In the absence of metastatic disease, ganglioneuroma in older children is indistinguishable from neuroblastoma on imaging. When histological assessment is unclear, biopsy is not feasible or the diagnosis is uncertain, MIBG scanning should be considered. MIBG will demonstrate primary tumor uptake in over half of such cases, confirm the presence of a neural crest tumor, and simultaneously screen for metastases.

5.3 Lymphangiomatosis

Lymphangiomatosis is a rare disease characterized by is proliferation of complex anastomosing lymphatic channels with secondary lymphatic dilation. The disease is believed to be congenital and the majority of cases are diagnosed in childhood. It may present with single organ or multiorgan involvement, and most frequently involves the thorax (Wunderbaldinger et al. 2000).

Clinical presentation depends on the sites and extent of disease involvement, and may include dyspnea, wheezing, chest pain, or neck swelling. Initial misdiagnosis as asthma or other respiratory diseases is common (Satria et al. 2011). Diffuse, bilateral symmetric interlobular and peribronchovascular thickening, which may be smooth or nodular, is seen on CT, often with an upper lobe predominance (Swenson et al. 1995). CT also reveals edematous mediastinal soft tissues, a very distinctive finding (Fig. 16). MRI shows hyperintense signal on T2-weighted images and heterogeneous

Table 2 Description of IDRFs applicable to thoracic neuroblastic tumors

Anatomic Region	Description of IDRFs
Multiple body compartments	Ipsilateral tumor extension within two adjacent body compartments (e.g. neck and chest, chest and abdomen)
Cervicothoracic junction	Tumor encasing brachial plexus roots Tumor encasing subclavian vessels, vertebral artery, and/or carotid artery Tumor compressing trachea
Thorax	Tumor encasing aorta and/or major branches Tumor compressing trachea and/or principal bronchi Lower mediastinal tumor infiltrating costovertebral junction between T9 and T12 vertebral levels
Thoracoabdominal junction	Tumor encasing aorta and/or vena cava
Intraspinal tumor extension	Intraspinal tumor extension provided that more than one-third of spinal canal in axial plane is invaded, the perimedullary leptomeningeal spaces are not visible, or the spinal cord signal intensity is abnormal
Infiltration of adjacent organs and structures	Pericardium, diaphragm

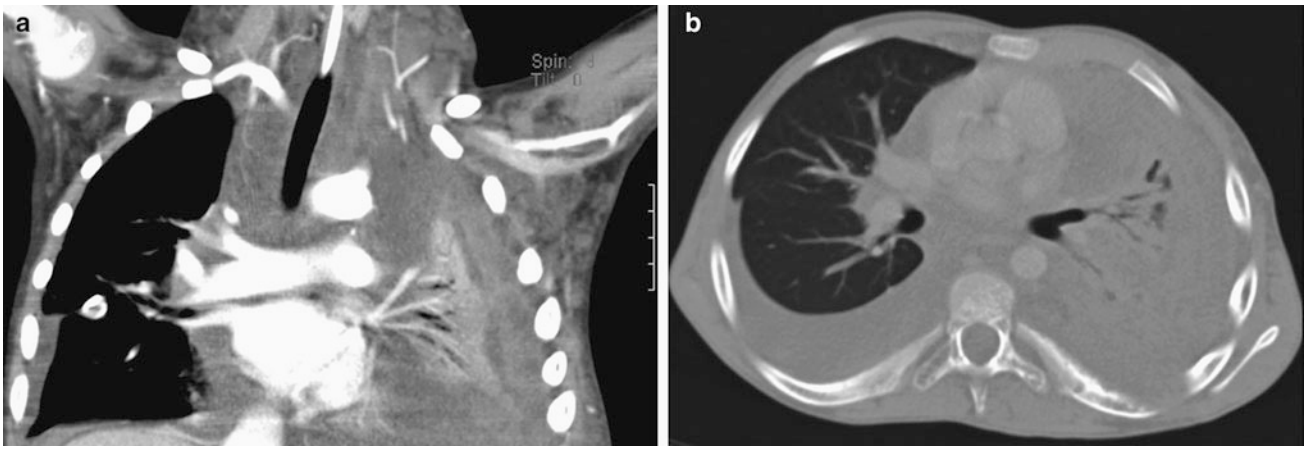

Fig. 16 Lymphangiomatosis. **a** Coronal contrast-enhanced chest CT image shows a collapsed left lung enveloped by edematous tissue along the pleura that extends into the left axilla and mediastinum. **b** Axial chest CT image in bone windows from the same patient reveals ill-defined lucencies in a thoracic vertebra and a posterior left rib

enhancement of abnormal soft tissue in the mediastinal and paraspinous regions without extension into the neural foramina or spinal canal (Shah et al. 2011). Pleural or pericardial infiltration is frequently present and chylous effusions are common (Aviv and McHugh 2000). Common extrathoracic findings include osteolytic bone lesions, enlargement of the spleen, and cystic splenic lesions.

The clinical course and prognosis are variable. Some cases show inexorable progression, while others spontaneously arrest. Although lymphangiomatosis is histologically benign, patients with chylothorax associated with osteolytic lesions have a notably poor prognosis. Attempts at surgical excision are rarely curative due to the infiltrative nature of the disease, and may exacerbate chylous leakage. Sclerotherapy, drainage procedures, and medical therapy with vincristine, sirolimus, interferon α-2b, or propanolol are palliative or temporizing measures. Intractable effusions, infection, and cardiorespiratory failure frequently supervene (Satria et al. 2011).

A novel subtype, Kaposiform lymphangiomatosis, has recently been described, and is characterized by spindled endothelial cells accompanying the malformed lymphatic channels, along with a propensity for hemorrhage and hematologic abnormalities similar to the Kasabach–Merritt phenomenon seen with Kaposiform hemangioendothelioma. As with classic lymphangiomatosis, the mediastinum, lungs, pleura, bones, and spleen are most commonly involved. The overall survival is reported at 34 % with mean interval of 2.75 years between diagnosis and death (Croteau et al. 2013).

5.4 Esophageal Leiomyomatosis

Although quite rare, leiomyomas are the most common benign tumor of the esophagus. Esophageal leiomyomas are more likely to be multiple or diffuse in children than in adults, and pediatric esophageal leiomyomatosis is associated with Alport syndrome. The involved esophagus demonstrates marked circumferential wall thickening that leads to dysphagia. In severe cases, mass effect on the adjacent airway can produce respiratory symptoms (Guest et al. 2000).

6 Conclusion

Non-neoplastic masses and pulmonary metastases from extracranial solid tumors are far more common than primary pulmonary neoplasms in childhood. Although rare, primary pulmonary neoplasms are often malignant and can cause considerable morbidity and mortality from mass effect, tissue invasion, and metastatic disease. Mesenchymal neoplasms are more common than epithelial neoplasms in the pediatric lung, unlike in adults, and some of these neoplasms are associated with predisposing genetic syndromes or certain infections. While lymphoma is the most common mediastinal malignancy, germ cell, neuroblastic, and other mediastinal tumors also manifest with distinctive features that are important to recognize for appropriate management. Many of these tumors are detectable on chest radiography, but chest CT remains the primary imaging modality used to formulate a differential diagnosis for these tumors, define anatomy for preoperative planning, assess tumor response to therapy, and survey for recurrent disease, with MRI and nuclear medicine studies playing a complementary role.

References

Adams GA, Shochat SJ, Smith EI, Shuster JJ, Joshi VV, Altshuler G, Hayes FA, Nitschke R, McWilliams N, Castleberry RP (1993) Thoracic neuroblastoma: a Pediatric Oncology Group study. J Pediatr Surg 28:372–377

Alobeid B, Beneck D, Sreekantaiah C, Abbi RK, Slim MS (1997) Congenital pulmonary myofibroblastic tumor: a case report with cytogenetic analysis and review of the literature. Am J Surg Pathol 21:610–614

Alper F, Kaynar H, Kantarci M, Onbas O, Polat P, Erdogan F, Akgun M, Okur A (2005) Trichoptysis caused by intrapulmonary teratoma: computed tomography and magnetic resonance imaging findings. Australas Radiol 49:53–56

Al-Qahtani AR, Di Lorenzo M, Yazbeck S (2003) Endobronchial tumors in children: institutional experience and literature review. J Pediatr Surg 38:733–736

Andronikou S, Kader E (2001) Bronchial mucoepidermoid tumour in a child with organomegaly due to secondary amyloidosis: case report and review of the literature. Pediatr Radiol 31:348–350

Aviv R, McHugh K (2000) Mechanisms of chylous effusions in lymphangiomatosis. AJR Am J Roentgenol 175:1191

Balsam D, Segal S (1992) Two smooth muscle tumors in the airway of an HIV-infected child. Pediatr Radiol 22:552–553

Bastos MD, Lee EY, Strauss KJ, Zurakowski D, Tracy DA, Boiselle PM (2009) Motion artifact on high-resolution CT images of pediatric patients: comparison of volumetric and axial CT methods. AJR Am J Roentgenol 193:1414–1418

Brader P, Abramson SJ, Price AP, Ishill NM, Zabor EC, Moskowitz CS, LaQuaglia MP, Ginsberg MS (2011) Do characteristics of pulmonary nodules on computed tomography in children with known osteosarcoma help distinguish whether the nodules are malignant or benign? J Pediatr Surg 46:729–735

Brady SL, Moore BM, Yee BS, Kaufman RA (2014) Pediatric CT: implementation of ASIR for substantial radiation dose reduction while maintaining pre-ASIR image noise. Radiology 270:223–231

Brisse HJ, McCarville BM, Granata C, Krug KB, Wootton-Gorges SL, Kanegawa K, Giammarile F, Schmidt M, Shulkin BL, Matthay KK, Lewington VJ, Sarnacki S, Hero B, Kaneko M, London WB, Pearson AD, Cohn SL, Monclair T (2011) Guidelines for imaging and staging of neuroblastic tumors: consensus report from the International Neuroblastoma Risk Group Project. Radiology 261:243–257

Buchmann I, Henze M, Engelbrecht S, Eisenbut M, Runz A, Schafer M, Schilling T, Haufe S, Herrman T, Haberkorn U (2007) Comparison of 68 Ga-DOTATOC PET and In111-DTPAOC (Octreoscan) SPECT in patients with neuroendocrine tumours. Eur J Nucl Med Mol Imaging 34:1617–1626

Buyukavci M, Atlas S, Salman B, Eren S (2006) An aggressive childhood tumor mimicking pleural empyema: pleuropulmonary blastoma. J Pediatr Hematol Oncol 28:257–259

Chadwick EG, Connor EJ, Hanson IC, Joshi VV, Abu-Farsakh H, Yogev R, McSherry G, McClain K, Murphy SB (1990) Tumors of smooth muscle origin in HIV-infected children. JAMA 263:3182–3184

Chong S, Lee KS, Chung MJ, Han J, Kwon OJ, Kim TS (2006) Neuroendocrine tumors of the lung: clinical, pathologic, and imaging findings. Radiographics 26:41–57

Choi S-J, Lee JS, Song KS, Lim T-H (1998) Mediastinal teratoma: CT differentiation of ruptured and unruptured tumors. AJR Am J Roentgenol 171:591–594

Cistaro A, Lopci E, Gastaldo L, Fania P, Del Prever AB, Fagioli F (2012) The role of 18F-FDG PET/CT in the metabolic characterization of lung nodules in pediatric patients with bone sarcoma. Pediatr Blood Cancer 59:1206–1210

Coakley FV, Cohen MD, Johnson MS, Gonin R, Hanna MP (1998) Maximum intensity projection images in the detection of simulated pulmonary nodules by spiral CT. Br J Radiol 71:135–140

Coffin CM, Hornick JL, Fletcher CD (2007) Inflammatory myofibroblastic tumor: comparison of clinicopathologic, histologic, and immunohistochemical features including ALK expression in atypical and aggressive cases. Am J Surg Pathol 31:509–520

Cohen MC, Kaschula RO (1992) Primary pulmonary tumors in childhood: a review of 31 years' experience and the literature. Pediatr Pulmonol 14:222–232

Connolly BL, Chait PG, Duncan DS, Taylor G (1999) CT guided percutaneous needle biopsy of small lung nodules in children. Pediatr Radiol 29:342–346

Cook JR, Hill DA, Humphrey PA, Pfeifer JD, El-Mofty SK (2000) Squamous cell carcinoma arising in recurrent respiratory papillomatosis with pulmonary involvement: emerging common pattern of clinical features and human papillomavirus serotype association. Mod Pathol 13:914–918

Cowie F, Corbett R, Pinkerton CR (1997) Lung involvement in neuroblastoma: incidence and characteristics. Med Pediatr Oncol 28:429–432

Croteau SE, Kozakewich HPW, Perez-Atayde AR, Fishman SJ, Alomari AI, Chaudry G, Mulliken JB, Trenor CC (2013) Kaposiform lymphangiomatosis: a distinct aggressive lymphatic anomaly. J Pediatr. doi: 10.1016/j.jpeds.2013.10.013 (Epub ahead of print)

Curtis JM, Lacey D, Smyth R, Carty H (1998) Endobronchial tumours in childhood. Eur J Radiol 29:11–20

Daldrup HE, Link TM, Wortler K, Reimer P, Rummeny EJ (1997) MR imaging of thoracic tumors in pediatric patients. AJR Am J Roentgenol 170:1639–1644

den Bakker MA, Beverloo BH, van den Heuvel-Eibrink MM, Meeuwis CA, Tan LM, Johnson LA, French CA, van Leenders GJ (2009) NUT midline carcinoma of the parotid gland with mesenchymal differentiation. Am J Surg Pathol 33:1253–1258

Dehner LP (1994) Pleuropulmonary blastoma is THE pulmonary blastoma of childhood. Semin Diagn Pathol 11:144–151

Dehner LP, Watterson J, Priest J (1995) Pleuropulmonary blastoma: a unique intrathoracic-pulmonary neoplasm of childhood. Perspect Pediatr Pathol 18:214–226

Diederich S, Lenzen H, Windmann R, Puskas Z, Yelbuz TM, Henneken S, Klaiber T, Eameri M, Roos N, Peters PE (1999) Pulmonary nodules: experimental and clinical studies at low dose CT. Radiology 213:289–298

Diederich S, Hansen J, Wormanns D (2005) Resolving small pulmonary nodules: CT features. Eur Radiol 15:2064–2069

Diemel KD, Klippe HJ, Branseheid D (2009) Pulmonary metastasectomy for osteosarcoma: is it justified? Recent Results Cancer Res 179:183–208

Dishop MK, Kuruvilla S (2008) Primary and metastatic lung tumors in the pediatric population: a review and 25-year experience at a large children's hospital. Arch Pathol Lab Med 132:1079–1103

Dishop MK, McKay EM, Kreiger PA, Priest JR, Williams GM, Langston C, Jarzembowksi J, Suchi M, Dehner LP, Hill DA (2010) Fetal lung interstitial tumor (FLIT): a proposed newly recognized lung tumor of infancy to be differentiated from cystic pleuropulmonary blastoma and other developmental pulmonary lesions. Am J Surg Pathol 34:1762–1772

DuBois SG, London WB, Zhang Y, Matthay KK, Monclair T, Ambros PF, Cohn SL, Pearson A, Diller L (2008) Lung metastases in neuroblastoma at initial diagnosis: a report from the International Neuroblastoma Risk Group (INRG) project. Pediatr Blood Cancer 51:589–592

Dulmet EM, Macchiarini P, Suc B, Verley JM (1993) Germ cell tumours of the mediastinum: a 30 year experience. Cancer 72:1894–1901

Elidemir O, Kancherla BS, Schecter MG, McKenzie ED, Morales DL, Heinle JS, Mallory GB (2009) Post-transplant lymphoproliferative disease in pediatric lung transplant recipients: recent advances in monitoring. Pediatr Transplant 13:606–610

Foulkes WD, Bahubeshi A, Hamel N, Pasini B, Asioli S, Baynam G, Choong CS, Charles A, Frieder RP, Dishop MK, Graf N, Ekim M, Bouron-Dal Soglio D, Arseneau J, Young RH, Sabbaghian N, Srivastava A, Tischkowitz MD, Priest JR (2011) Extending the phenotypes associated with DICER1 mutations. Hum Mutat 32:1381–1384

French CA (2010) NUT midline carcinoma. Cancer Genet Cytogenet 203:16–20

French CA, Kutok JL, Faquin WC, Toretsky JA, Antonescu CR, Griffin CA, Nose V, Vargas SO, Moschovi M, Tzortzatou-Stathopoulou F, Miyoshi I, Perez-Atayde AR, Aster JC, Fletcher JA (2004) Midline carcinoma of children and young adults with NUT rearrangement. J Clin Oncol 22:4135–4139

Fuchs J, Seitz G, Handgretinger R, Schafer J, Warmann SW (2012) Surgical treatment of lung metastases in patients with embryonal pediatric solid tumors: an update. Semin Pediatr Surg 21:79–87

Goel P, Panda S, Srinivas M, Kumar D, Seith A, Ahuja A, Sarkar C, Chowdhury S, Agarwala S (2010) Pleuropulmonary blastoma with intrabronchial extension. Pediatr Blood Cancer 54:1026–1028

Gross E, Chen MK, Hollabaugh RS, Joyner RE (1996) Tracheal hamartoma: report of a child with a neck mass. J Pediatr Surg 31:1584–1585

Gruden JF, Ouanounou S, Tigges S, Norris SD, Klausner TS (2002) Incremental benefit of maximum-intensity-projection images on observer detection of small pulmonary nodules revealed by multidetector CT. AJR Am J Roentgenol 179:149–157

Grundy PE, Green DM, Dirks AC, Berendt AE, Breslow NE, Anderson JR, Dome JS (2012) Clinical significance of pulmonary nodules detected by CT and not CXR in patients treated for favorable histology Wilms tumor on national Wilms tumor studies-4 and -5: a report from the Children's Oncology Group. Pediatr Blood Cancer 59:631–635

Guest AR, Strouse PJ, Hiew CC, Arca M (2000) Progressive esophageal leiomyomatosis with respiratory compromise. Pediatr Radiol 30:247–250

Guillerman RP, Voss SD, Parker BR (2011) Leukemia and lymphoma. Radiol Clin N Am 49:767–797

Hancock BJ, Di Lorenzo M, Youssef S, Yazbeck S, Marcotte JE, Collin PP (1993) Childhood primary pulmonary neoplasms. J Pediatr Surg 28:1133–1136

Hartman GE, Shochat SJ (1983) Primary pulmonary neoplasms of childhood: a review. Ann Thorac Surg 36:108–119

Hedlund GL, Navoy JF, Galliani CA, Johnson WH Jr (1999) Aggressive manifestations of inflammatory pseudotumor in children. Pediatr Radiol 29:112–116

Helm EJ, Silva CT, Roberts HC, Manson D, Seed MT, Amaral JG, Babyn PS (2009) Computed-aided detection for the identification of pulmonary nodules in pediatric oncology patients: initial experience. Pediatr Radiol 39:685–693

Horikoshi T, Kikuchi A, Matsumoto Y, Tatematsu M, Takae K, Ogiso Y, Nakayama M, Unno N (2005) Fetal hydrops associated with congenital pulmonary myofibroblastic tumor. J Obstet Gynaecol Res 31:552–555

Huang Y, Xu DM, Jirapatnakul A, Reeves AP, Farooqi A, Zhang Lj, Giunta S, Zulueta J, Aye R, Miller A, Mendelson DS, Aylesworth C, Sheppard B, Klingler K, Yankelevitz DF, Henschke CI (2011) CT- and computer-based features of small hamartomas. Clin Imaging 35:116–122

Huppmann AR, Coffin CM, Hoot AC, Kahwash S, Pawel BR (2011) Congenital peribronchial myofibroblastic tumor: comparison of fetal and postnatal morphology. Pediatr Dev Pathol 14:124–129

Indolfi P, Bisogno G, Casale F, Cecchetto G, De Salvo G, Ferrari A, Donfrancecsco A, Donofrio V, Martone A, Di Martino M, Di Tullio MT (2007) Prognostic factors in pleuro-pulmonary blastoma. Pediatr Blood Cancer 48:318–323

Janik JS, Janik JP, Lovell MA, Hendrickson RJ, Bensard DD, Grefe BS (2003) Recurrent inflammatory pseudotumors in children. J Pediatr Surg 38:1491–1495

Jeung MY, Gasser B, Gangi A, Charneau D, Ducroq X, Kessler R, Quiox E, Roy C (2002) Bronchial carcinoid tumors of the thorax: spectrum of radiologic findings. Radiographics 22:351–365

Kammen BF, Matthay KK, Pacharn P, Gerbing R, Brasch RC, Gooding CA (2001) Pulmonary metastases at diagnosis of neuroblastoma in pediatric patients: CT findings and prognosis. AJR Am J Roentgenol 176:755–759

Kaste SC, Pratt CB, Cain AM, Jones-Wallace DJ, Rao BN (1999) Metastases detected at the time of diagnosis of primary pediatric extremity osteosarcoma: imaging features. Cancer 86:1602–1608

Katz SL, Das P, Ngan BY, Manson D, Pappo AS, Sweezey NB, Solomon MP (2005) Remote intrapulmonary spread of recurrent

respiratory papillomatosis with malignant transformation. Pediatr Pulmonol 39:185–188

Kayton ML, Huvos AG, Casher J, Abramson SJ, Rosen NS, Wexler LH, Meyers P, LaQuaglia MP (2006) Computed tomographic scan of the chest underestimates the number of metastatic lesions in osteosarcoma. J Pediatr Surg 41:200–206

Kawel N, Seifert B, Luetolf M, Boehm T (2009) Effect of slab thickness on the CT detection of pulmonary nodules: use of sliding thin-slab maximum intensity projection and volume rendering. AJR Am J Roentgenol 192:1324–1329

Kim TS, Lee KS, Han J, Im JG, Seo JB, Kim JS, Kim HY, Han SW (1999) Mucoepidermoid carcinoma of the tracheobronchial tree: radiographic and CT findings in 12 patients. Radiology 212:643–648

Kim Y, Park HY, Cho J, Han J, Cho EY (2013) Congenital peribronchial myofibroblastic tumor: a case study and literature review. Korean J Pathol 47:172–176

Kleis M, Daldrup-Link H, Matthay K, Goldsby R, Lu Y, Schuster T, Schreck C, Chu PW, Hawkins RA, Franc BL (2009) Diagnostic value of PET/CT for the staging and restaging of pediatric tumors. Eur J Nucl Med Mol Imaging 36:23–36

Kocaoglu M, Bulakbasi N, Soylu K, Demirbag S, Tayfun C, Somuncu I (2006) Thin section axial multidetector computed tomography and multiplanar reformatted imaging of children with suspected foreign body: is virtual bronchoscopy overemphasized? Acta Radiol 47:746–751

Koopmans KP, Neels OC, Kema IP, Elsinga PH, Sluiter WJ, Vanghillewe K, Brouwers AH, Jager PL, de Vries EG (2008) Improved staging of patients with carcinoid and islet cell tumors with 18F–dihydroxy-phenyl-alanine and 11C-5-hydroxy-tryptophan positron emission tomography. J Clin Oncol 26:1489–1495

Koujok K, Ruiz RE, Hernandez RJ (2005) Myofibromatosis: imaging characteristics. Pediatr Radiol 35:374–380

Kramer SS, Wehunt WD, Stocker JT, Kashima H (1985) Pulmonary manifestations of juvenile laryngotracheal papillomatosis. AJR Am J Roentgenol 144:687–694

Kuhns LR, Roubal S (1995) Should intravenous contrast be used for chest CT in children with nonlymphomatous extrathoracic malignancies? Pediatr Radiol 25(Suppl 1):S184–S186

Lal DR, Clark I, Shalkow J, Downey RJ, Shorter NA, Klimstra DS, La Quaglia MP (2005) Primary epithelial lung malignancies in the pediatric population. Pediatr Blood Cancer 45:683–686

Lazar DA, Cass DL, Dishop MK, Adam K, Olutoye OA, Ayres NA, Cassady CI, Olutoye OO (2011) Fetal lung interstitial tumor: a cause of late gestation fetal hydrops. J Pediatr Surg 46:1263–1266

Letourneau PA, Xiao L, Harting MT, Lally KP, Cox CS Jr, Andrassy RJ, Hayes-Jordan AA (2011) Location of pulmonary metastasis in pediatric osteosarcoma is predictive of outcome. J Pediatr Surg 46:1333–1337

Levine E, Freneaux P, Schleiermacher G, Brisse H, Pannier S, Teissier N, Mesples B, Orbach D (2012) Risk-adapted therapy for infantile myofibromatosis in children. Pediatr Blood Cancer 59:115–120

Mas Estelles F, Andres V, Vallcanera A, Muro D, Cortina H (1995) Plasma cell granuloma of the lung in childhood: atypical radiologic findings and association with hypertrophic osteoarthropathy. Pediatr Radiol 25:369–372

Maturen KE, Blane CE, Strouse PJ, Fitzgerald JT (2004) Pulmonary involvement in pediatric lymphoma. Pediatr Radiol 34:120–124

McCahon E (2006) Lung tumours in children. Paediatr Respir Rev 7:191–196

McCarville MB, Lederman HM, Santana VM, Daw NC, Shochat SJ, Li CS, Kaufman RA (2006) Distinguishing benign from malignant pulmonary nodules with helical chest CT in children with malignant solid tumors. Radiology 239:514–520

McClain KL, Leach CT, Jenson HB, Joshi VV, Pollock BH, Parmley RT, DiCarlo FJ, Chadwick EG, Murphy SB (1995) Association of Epstein-Barr virus with leiomyosarcomas in children with AIDS. N Engl J Med 332:12–18

McHugh K, Disini L (2011) Commentary: for the children's sake, avoid non-contrast CT. Cancer Imaging 11:16–18

Mergan F, Jaubert F, Sauvat F, Hartmann O, Lortat-Jacob S, Revillon Y, Nihoul-Fekete C, Sarnacki S (2005) Inflammatory myofibroblastic tumor in children: clinical review with anaplastic lymphoma kinase, Epstein-Barr virus and human herpes virus 8 detection analysis. J Pediatr Surg 40:1581–1586

Miniati DN, Chintagumpala M, Langston C, Dishop MK, Olutoye OO, Nuchtern JG, Cass DL (2006) Prenatal presentation and outcome of children with pleuropulmonary blastoma. J Pediatr Surg 41:66–71

Morini F, Quattrucci S, Cozzi DA, Tancredi G, Cicconi AM, Guidi R, Midulla F (2003) Bronchial adenoma: an unusual cause of recurrent pneumonia in childhood. Ann Thorac Surg 76:2085–2087

Murrell Z, Dasgupta R (2013) What predicts the risk of recurrent lung metastases. J Pediatr Surg 48:1020–1024

Murrell Z, Dickie B, Dasgupta R (2011) Lung nodules in pediatric oncology patients: a prediction rule for when to biopsy. J Pediatr Surg 46:833–837

Newman B (2011) Thoracic neoplasms in children. Radiol Clin North Am 49:633–664

Pai S, Eng HL, Lee SY, Hsaio CC, Huang WT, Huang SC, Hill DA, Dehner LP, Priest JR (2007) Correction: pleuropulmonary blastoma, not rhabdomyosarcoma in a congenital lung cyst. Pediatr Blood Cancer 48:370–371

Parham DM, Alaggio R, Coffin CM (2012) Myogenic tumors in children and adolescents. Pediatr Dev Pathol 15:211–238

Park KY, Kim SJ, Noh TW, Cho SH, Lee DY, Paik HC, Ryu YH (2008) Diagnostic efficacy and characteristic feature of MRI in pulmonary hamartoma: comparison with CT, specimen MRI and pathology. J Comput Assist Tomogr 32:919–925

Paulussen M, Ahrens S, Craft AW, Dunst J, Frohlich B, Jabar S, Rube C, Winkelmann W, Wissing S, Zoubek A, Jurgens H (1998) Ewing's tumour with primary lung metastases: survival analysis of 114 (European Intergroup) Cooperative Ewing's Sarcoma Studies patients. J Clin Oncol 16:3044–3052

Pickhardt PJ, Siegel MJ, Hayashi RJ, Kelly M (2000) Post-transplantation lymphoproliferative disorder in children: clinical, histopathologic, and imaging features. Radiology 217:16–25

Pipavath SN, Manchanda V, Lewis DH, Schmidt RA, Martins RG, Godwin JD (2008) 18F FDG-PET/CT findings in recurrent respiratory papillomatosis. Ann Nucl Med 22:433–436

Polsani A, Braithwaite KA, Alazraki AL, Abramowsky C, Shehata BM (2012) NUT midline carcinoma: an imaging case series and review of literature. Pediatr Radiol 42:205–210

Priest JR (2012) Pleuropulmonary blastoma. In: Schneider DTBI, Olson TA, Ferrari A (eds) Rare tumors in children and adolescents, pediatric oncology. Springer, Berlin, pp 213–221

Priest JR, McDermott MB, Bhatia S, Watterson J, Manivel JC, Dehner LP (1997) Pleuropulmonary blastoma: a clinicopathologic study of 50 cases. Cancer 80:147–161

Priest JR, Hill AD, Williams GM, Moertel CL, Messinger Y, Finkelstein MJ, Dehner LP (2006) Type I pleuropulmonary blastoma: a report from the International Pleuropulmonary Blastoma Registry. J Clin Oncol 24:4492–4498

Priest JR, Williams GM, Hill DA, Dehner LP, Jaffe A (2009) Pulmonary cysts in early childhood and the risk of malignancy. Pediatr Pulmonol 44:14–30

Priest JR, Andic D, Arbucke S, Gonzalez-Gomez I, Hill DA, Williams G (2011) Great vessel/cardiac extension and tumor embolism in

pleuropulmonary blastoma: a report from the International Pleuropulmonary Blastoma Registry. Pediatr Blood Cancer 56:604–609
Rabah R, Lancaster WD, Thomas R, Gregoire L (2001) Human papillomavirus-11-associated recurrent respiratory papillomatosis is more aggressive than human papillomavirus-6-associated disease. Pediatr Dev Pathol 4:68–72
Rizzardi G, Marulli G, Calabrese F, Rugge M, Rebusso A, Sartori F, Rea F (2009) Bronchial carcinoid tumours in children: surgical treatment and outcome in a single institution. Eur J Pediatr Surg 19:228–231
Rodriguez FJ, Aubry MC, Tazelaar HD, Slezak J, Carney JA (2007) Pulmonary chondroma: a tumor associated with Carney triad and different from pulmonary hamartoma. Am J Surg Pathol 31:1844–1853
Rosenbaum DG, Feldstein JT, Price AP, Meyers P, Abramson S (2012) Radiologic features of NUT midline carcinoma in an adolescent. Pediatr Radiol 42:249–252
Sasaka K, Kurihara Y, Nakajima Y, Seto Y, Endo I, Ishikawa T, Takagi M (1998) Spontaneous rupture: a complication of benign mature teratomas of the mediastinum. AJR Am J Roentgenol 170:323–328
Satria MN, Pacheco-Rodriguez G, Moss J (2011) Pulmonary lymphangiomatosis. Lymphat Res Biol 9:191–193
Schiavetti A, Indolfi P, Hill DA, Priest JR (2009) Primary pulmonary rhabdomyosarcoma in childhood: clinic-biologic features in two cases with review of the literature—erratum. Pediatr Blood Cancer 52:146
Seemayer TA, Harper JL, Shickell D, Gross TG (1997) Cytodifferentiation of a Wilms' tumor pulmonary metastasis: theoretic and clinical implications. Cancer 79:1629–1634
Seifert RP, McNab P, Sexton WJ, Sawczyn KK, Smith P, Coppola D, Bui MM (2012) Rhabdomyomatous differentiation in Wilms tumor pulmonary metastases: a case report and literature review. Ann Clin Lab Sci 42:409–416
Shah V, Shah S, Barnacle A, Sebire NJ, Brock P, Harper JI, McHugh K (2011) Mediastinal involvement in lymphangiomatosis: a previously unreported MRI sign. Pediatr Radiol 41:985–992
Siegel MJ, Ishwaran HI, Fletcher BD, Meyer JS, Hoffer FA, Jaramillo D, Hernandez RJ, Roubal SE, Siegel BA, Caudry DJ, McNeil BJ (2002) Staging of neuroblastoma at imaging: report of the Radiology Diagnostic Oncology Group. Radiology 223:168–175
Siegel MJ, Lee EY, Sweet SC, Hildebolt C (2003) CT of posttransplantation lymphoproliferative disorder in pediatric recipients of lung allografts. AJR Am J Roentgenol 181:1125–1131
Silva CT, Amaral JG, Moineddin R, Doda W, Babyn PS (2010). CT characteristics of lung nodules present at diagnosis of extrapulmonary malignancy in children. AJR Am J Roentgenol 194:772–8
Siminovich M, Galluzzo L, Lopez J, Lubieniecki F, de Davila MT (2012) Inflammatory myofibroblastic tumor of the lung in children: anaplastic lymphoma kinase (ALK) expression and clinico-pathological correlation. Pediatr Dev Pathol 15:179–186
Slade I, Bacchelli C, Davies H, Murray A, Abbaszadeh F, Hanks S, Barfoot R, Burke A, Chisholm J, Hewitt M, Jenkinson H, King D, Morland B, Pizer B, Prescott K, Saggar A, Side L, Traunecker H, Vaidya S, Ward P, Futreal PA, Vujanic G, Nicholson AG, Sebire N, Turnbull C, Priest JR, Pritchard-Jones K, Houlston R, Stiller C, Stratton MR, Douglas J, Rahman N (2010) DICER1 syndrome: clarifying the diagnosis, clinical features and management implications of a pleiotropic tumour predisposition syndrome. J Med Genet 48:273–278
Smets AM, van Tinteren H, Bergeron C, De Camargo B, Graf N, Pritchard-Jones K, de Kraker J (2012) The contribution of chest CT-scan at diagnosis in children with unilateral Wilms' tumour. Results of the SIOP 2001 study. Eur J Cancer 48:1060–1065
Soldatski I, Onufrieva E, Steklov A, Schepin NV (2005) Tracheal, bronchial and pulmonary papillomatosis in children. Laryngoscope 115:1848–1854
Stratakis CA, Carney JA (2009) The triad of paragangliomas, gastric stromal tumours and pulmonary chondromas (Carney triad), and the dyad of paragangliomas and gastric stromal sarcomas (Carney-Stratakis syndrome): molecular genetics and clinical implications. J Intern Med 266:43–52
Strollo DC, Rosado de Christenson ML, Jett JR (1997) Primary mediastinal tumors. Part 1: tumors of the anterior mediastinum. Chest 112:511–522
Swenson SJ, Hartman TE, Mayo JR, Colby TV, Tazelaar HD, Muller NL (1995) Diffuse pulmonary lymphangiomatosis: CT findings. J Comput Assist Tomogr 19:348–352
Takayama Y, Yabuuchi H, Matsuo Y, Soeda H, Okafuji T, Kamitani T, Kinoshita Y, Kubokura N, Sakai S, Oda Y, Hatakenaka M, Honda H (2008) Computed tomographic and magnetic resonance features of inflammatory myofibroblastic tumor of the lung in children. Radiat Med 26:613–617
Tanaka M, Kato K, Gomi K, Yoshida M, Niwa T. Aida N, Kigasawa H, Ohama Y, Tanaka Y (2012) NUT midline carcinoma: report of 2 cases suggestive of pulmonary origin. Am J Surg Path 36:381-388
Travis WD, Dehner LP, Manabe T, Tazelaar HD (2004) Congenital peribronchial myofibroblastic tumor. In: Travis WD, Brambilla E, Muller-Hermelink HK, Harris CC (eds) World Health Organization classification of tumours: pathology and genetics of tumors of the lung, pleura, thymus, and heart. IARC Press, Lyon, pp 102–103
Tronc F, Conter C, Perrine MB, Bossard N, Remontet L, Orsini A, Gamondes JP, Louis D (2008) Prognostic factors and long-term results of pulmonary metastasectomy for pediatric histologies. Eur J Cardiothorac Surg 34:1240–1246
Verbeke JIM, Verbene AAPH, den Hollander JC, Robben SGF (1999) Inflammatory myofibroblastic tumour of the lung manifesting as progressive atelectasis. Pediatr Radiol 29:816–819
Verschuur A, Van Tinteren H, Graf N, Bergeron C, Sandstedt B, de Kraker J (2012) Treatment of pulmonary metastases in children with stage IV nephroblastoma with risk-based use of pulmonary radiotherapy. J Clin Oncol 30:3533–3539
Wang CW, Teng YH, Huang CC, Wu YC, Chao YK, Wu CT (2013) Intrapulmonary lymph nodes: computed tomography findings with histopathologic correlations. Clin Imaging 37:487–492
Wang LT, Wilkins EW Jr, Bode HH (1993) Bronchial carcinoid tumors in pediatric patients. Chest 103:1426–1428
Warmann SW, Nourkami N, Fruhwald M, Leuschner I, Schenk JP, Fuchs J, Graf N (2012) Primary lung metastases in pediatric malignant non-Wilms renal tumors: data from SIOP 93–01/GPOH and SIOP 2011/GPOH. Klin Padiatr 224:148–152
Wilde GE, Moore DJ, Bellah RD (2005) Posttransplantation lymphoproliferative disorder in pediatric recipients of solid organ transplants: timing and location of disease. AJR Am J Roentgenol 185:1335–1341
Williams SD, Jamieson DH, Prescott CA (1994) Clinical and radiological features in three cases of pulmonary involvement from recurrent respiratory papillomatosis. Int J Pediatr Otorhinolaryngol 30:71–77
Wu M, Wang Q, Xu XF, Xiang JJ (2011) Bronchial mucoepidermoid carcinoma in children. Thorac Cardiovasc Surg 59:443–445
Wunderbaldinger P, Paya P, Partik B, Turetschek K, Hormann M, Horcher E, Bankier AA (2000) CT and MR imaging of generalized cystic lymphangiomatosis in pediatric patients. AJR Am J Roentgenol 174:827–832
Xi JJ, Jiang W, Lu SH, Zhang CY, Fan H, Wang Q (2012) Primary pulmonary mucoepidermoid carcinoma: an analysis of 21 cases. World J Surg Oncol 10:232

Yalcin B, Demir HA, Tanyel FC, Akcoren Z, Varan A, Akyuz C, Kutluk T, Buyukpamukcu M (2012) Mediastinal germ cell tumors in childhood. Pediatr Hematol Oncol 29:633–642

Yousem SA, Tazelaar HD, Manabe T, Dehner LP (2004) Inflammatory myofibroblastic tumor. In: Travis WD, Brambilla E, Muller-Hermelink HK, Harris CC (eds) World Health Organization classification of tumours: pathology and genetics of tumors of the lung, pleura, thymus, and heat. IARC Press, Lyon, pp 105–106